UNIVERSITÀ POLITECNICA DELLE MARCHE

Master of Science Course in ENVIRONMENTAL ENGINEERING

UAV-based hydro-geomechanical analysis of an unstable rock sea cliff in Ancona (Marche Region, central Italy)

ADVISOR:

Mammoliti Elisa

STUDENT:

D'Antonio Lorenzo

CO-ADVISORS:

Tazioli Alberto

Pepi Alessandro

A.Y. 2022/2023

Ai miei genitori e mio fratello, per aver sempre creduto in me.

A Francesca, per essere sempre al mio fianco nella vita di tutti i giorni, per avermi supportato e sopportato in ogni momento.

Agli amici di una vita, per tutti i bei momenti passati insieme, so che ci sarete sempre.

Ai nonni, Gilberto e Pasquina, maestri di vita.

Acknowledgements

I would like to thank my supervisors for helping and supporting me in this thesis work:

Prof.ssa Elisa Mammoliti, Prof. Alberto Tazioli, Dr. Alessandro Pepi, Dr. Davide Fronzi

Special thanks also go to Mirko Francioni, reasercher at Univesrity of Urbino, for the support in the investigation of the area with the drone.

I also thank the department of “Scienze e Ingegneria della Materia e Urbanistica" of the Marche Polytechnic University for giving me all the help possible in this internship and thesis.

Summary

List of Figures

List of Tables

Abstract

Due to its geological, morphological, and hydrographic characteristics, Italy is naturally predisposed to instability. Landslides, floods, coastal erosion are frequent phenomena in our peninsula, especially along the Apennines and in the pre-Alpine belt. On one side the beauty and heterogeneity of the landscapes, on the other the geo-structural instability. In this context, the scientific literature presents many works on the triggers of rock landslides and, among these, the flow of groundwater through the fracturing system certainly plays a fundamental role. Thus, the investigation, analysis, and interpretation of the fracturing system of a rocky slope turns out to be a complex but crucial topic in the field of engineering geology, as the distribution, connectivity and opening of fractures govern the amount and movements of water within the rock volume. However, due to the inaccessibility of some areas, it is not always possible to investigate the entire rocky outcrop, or at least not by traditional methods. In this thesis the integration of an innovative method of hydro-geomechanical analysis based on the use of the drone (unmanned aerial vehicle, UAV) is proposed, combined with the traditional geomechanical method through one-dimensional scanlines. The area under study is in a portion of the Passetto cliff (Ancona, Marche), strongly affected by rockfall phenomena. Through the integration of the photogrammetric technique with drone and scanline, a large number of data were obtained and analysed, in order to create a 3D model of the sea cliff. Starting from the 3D model, two sampling windows representative of the entire area were considered, useful for analysing the fracturing system with the creation of a Discrete Fracture Network (DFN), useful to calculate the hydraulic conductivity of fractures. In order to validate the methodology, the results obtained from this approach were then integrated with a previous thesis work conducted in the same site and based on the use of artificial tracers.

Riassunto

Per le sue caratteristiche geologiche, morfologiche e idrografiche, l'Italia è naturalmente predisposta al dissesto idrogeologico; sempre più frequentemente sentiamo parlare di frane, alluvioni, erosione costiera nella nostra penisola, specialmente lungo gli Appennini e nella fascia pre-Alpina. Da un lato la bellezza e l'eterogeneità dei paesaggi, dall'altro la fragilità geo-strutturale. In questo contesto, la letteratura scientifica fornisce molti lavori riguardo le cause scatenanti delle frane in roccia, tra queste sicuramente gioca un ruolo fondamentale il flusso delle acque sotterranee attraverso il sistema di fratturazione. Quindi, l'indagine, l'analisi e l'interpretazione del sistema di fratturazione di un pendio roccioso risulta essere un tema complesso ma cruciale nel campo della geologia ingegneristica, in quanto la distribuzione, la connettività e l'apertura delle fratture governano la quantità e i movimenti d'acqua all'interno del volume roccioso. Tuttavia, a causa dell'inaccessibilità di alcune aree, non è sempre possibile indagare l'intero affioramento roccioso, o almeno non con metodi tradizionali. In questa tesi viene proposta l'integrazione di un metodo innovativo di analisi idro-geomeccanica basato sull'utilizzo del drone (unmanned aerial vehicle, UAV), abbinato al metodo geomeccanico tradizionale tramite scanline monodimensionale. L'area oggetto di studio è localizzata in una porzione della scogliera del Passetto (Ancona, Marche), fortemente interessata da fenomeni di caduta massi. Tramite l'integrazione della fotogrammetria con drone e scanline, sono stati ottenuti ed analizzati un elevato numero di dati, al fine di creare un modello 3D della scogliera. A partire dal modello sono state considerate due finestre di campionamento rappresentative dell'intera area, utili ad analizzare il sistema di fratturazione con la creazione di un Discrete Fracture Network (DFN) arrivando a calcolare la conducibilità idraulica delle fratture. I risultati ottenuti da questo tipo di approccio sono stati poi confrontati con un precedente lavoro di tesi basato sull'utilizzo di traccianti artificiali nello stesso sito, al fine di validare la metodologia.

1. Introduction

In low permeability rocks, the fracture network represents the major path for groundwater (Karra et al., 2018; Berkowitz et al., 2002; Adler et al., 2013; Worthington et al., 2022), which is strictly dependent on the hydraulic fracture connectivity (Krzeminska et al., 2012; 2013), the geometrical parameters (length, aperture, roughness) and fracture distribution (Camanni et al., 2021; Mayolle et al., 2021). Fractures within a rock mass are discontinuities that varies in orientation, geometry, size, length, thickness. Therefore, characterizing a fracture system is fundamental to understand the nature of an outcrop. The investigation, analysis and interpretation of fractures plays a fundamental role in different contexts: structural geology, hydrogeology, geotechnics, seismic risk, territorial planning.

In particular, the hydro-geomechanical investigation and the fracture analysis of a rock wall are fundamental to evaluate the dynamics of the phenomena of instability to which an area is particularly exposed (Price, 2016; Vasarhelyi et al., 2006; Althaus et al., 1994; Pan et al., 2020). In fact, water is one of the triggering factors for rockfalls, so modelling its circulation within a fractured rock system is of critical importance because high pressure on fractures, especially the ones with low shear strength, can easily affect the slope stability (Neuman et al., 2005; Wei et al., 2021). Basically, the more the fracturing grade, the more the groundwater circulation and the less block volume for rock slope instability; very fractured rocks can be more susceptible to failure and therefore cause irreparable damage to the surrounding environment and human health.

This study was conducted on a portion of the cliff of the Passetto beach, in Ancona (Marche Region, Italy), which is strongly affected by rock collapses during all the year.

An extensive literature review has been done considering the geological, geomorphological and geotechnical studies available for the study area. (Colosimo & Crescenti, 1973; Crescenti et al., 1978; Coltorti et al., 1987; Casagli et al., 1993; Fruzzetti et al., 2011; Iadanza et al., 2014; Aringoli et al. 2010, 2014; Montanari et al. 2016).

The mentioned area of Passetto, characterized in detail by the Schlier geological formation (Dubbini et al., 1991; Casagli et al., 1993), presents a high fractured rocky sea cliff, strongly affected by erosion from the sea and very steep slopes. All these factors influence the stability of this area, frequently causing rockfall.

Due to the high importance that fractures have in the field of engineering geology, a multi-method approach is used for their investigation: in order to get a more complete picture and analyse the entire rocky outcrop, especially in those inaccessible areas typical of coastal cliffs, traditional surveys via

scanline (Volatili et al., 2022; Jia et al., 2023) were combined with drone surveys (Unmanned Aerial Vehicle, UAV) improving fracture data collected (Massaro et al., 2018; Loiotine et al., 2019; Sturzenegger et al., 2009; Jabloska et al., 2021; Schilirò et al., 2022; Pitts et al., 2017).

In particular, the UAV photos acquired with the use of the drone and georeferenced through a total station were then processed within the software Agisoft Metashape to create a 3D model of the cliff. The 2D/3D digital-based outputs (dense point clouds, 3D model, orthophotos) were used to analyse and calculate within NetworkGT, a GIS tool (Nyberg et al.,2018), the fracture intensity, spacing (Mammoliti et al., 2022; Gigli et al., 2014; Riquelme et al., 2015) connectivity and size (Massaro et al., 2018; Loiotine et al., 2019; Walter et al., 2022).

A Discrete Fracture Network (DFN) was developed within the software MOVE following the fracture modelling module (Petroleum Experts Ltd., Edinburgh, UK), to create a 3D representation of the fracture system of the rock mass (Lei et al., 2017; Zhang et al., 2014; Romano et al., 2020; Giuffrida et al., 2020; Li et al., 2022; Smeraglia et al., 2021) and calculate the fracture conductivity. The results obtained were then compared with the results of a previous work based on tracer tests (Pepi, 2021).

A multi-level approach for the investigation of a rock mass is presented in this thesis, combining traditional geomechanical detection techniques with photogrammetric surveys from unmanned aerial vehicle. The main advantages that this methodology has brought to the study are highlighted, allowing the analysis of inaccessible areas, and obtaining a considerable amount of data. Through the use of specific softwares, the information obtained about the outcrop are processed and used to validate the methodology just described, providing realistic results and representing a further step forward in the field of geomechanics related to instability problems.

As a demonstration this thesis has contributed to the collection and interpretation of data of the published scientific paper named “3D Discrete Fracture Network Modelling from UAV Imagery Coupled with Tracer Tests to Assess Fracture Conductivity in an Unstable Rock Slope: Implications for Rockfall Phenomena” authored by Mammoliti et al. (2023).

2. State of the Art

2.1 Overview of landslide instability in Italy

Because of its geological, morphological, and hydrographic characteristics, Italy is naturally predisposed to instability: landslides, floods, coastal erosion, characterize our peninsula. In this framework, although Italy is one of the European countries mostly affected by landslides, with 625,000 landslides recorded in the Inventory of Landslides in Italy and affecting an area of almost 24,000 km^2 equal to 7.9% of the national territory, lack of landslide mitigation is evidenced from North to the South of Italy. Looking at the data collected in the period between 1970 and 2019 for landslide and flood events, Italy has 1,673 dead, 60 missing, 1,923 injured and 320,028 evacuees and homeless (CNR-IRPI data, 2020).

These are phenomena that fall within the concept of landslide instability.

To affect the frequency of the occurrence of these calamities, in fact, is not only the conformation of the territory but also the climate emergency of this historical period. Due to global warming in some areas of the planet, such as the Euro-Mediterranean area, extreme weather phenomena have intensified, often bringing with them sudden floods or rapid flows of mud and debris that compromise even more the structural stability of the territory.

In addition, to aggravate the situation, there is also the hand of human. Human action contributes greatly to aggravate the effects of landslides and floods, or even to activate them: deforestation of entire slopes, which exposes the soil to the direct action of rainwater; the abandonment of agricultural terraces, which for centuries have protected the mountain slopes; the construction of roads and major works such as viaducts, bridges and dams, which cut the slopes; excessive removal of sand and gravel from the riverbed, which increases the speed of the current; the construction of artificial embankments, which decrease the section of watercourses; the construction of buildings in the riverbeds or close to the banks.

To photograph the current situation of the hydrogeological risk of the country is Istat (Istituto nazionale di Statistica) with the report "Hydrogeological instability in Italy: hazard and risk indicators - 2021 Edition" based on 2020 data. According to the report, 7,423 municipalities (93.9% of the total) are at risk for landslides, floods or coastal erosion; 1.3 million inhabitants are at risk of landslides and 6.8 million are at risk of flooding.

In the figure below (Figure 1) we have a complete picture of the landslide situation in Italy, and specifically Ancona, considering the landslide index.

The indicator provides information on the number and distribution of landslides in Italy based on data contained in the Inventory of Landslides in Italy – IFFI (Inventario Fenomeni Franosi Italia). The Inventory is carried out by ISPRA (Istituto Superiore Protezione Ricerca Ambientale) and the regions and autonomous provinces; ISPRA has the function of guidance, coordination and control of activities, management of the database, production of national elaborations and statistics, dissemination of data; the regions and autonomous provinces have the fundamental role of collecting, storing, computerizing, and validating landslide data.

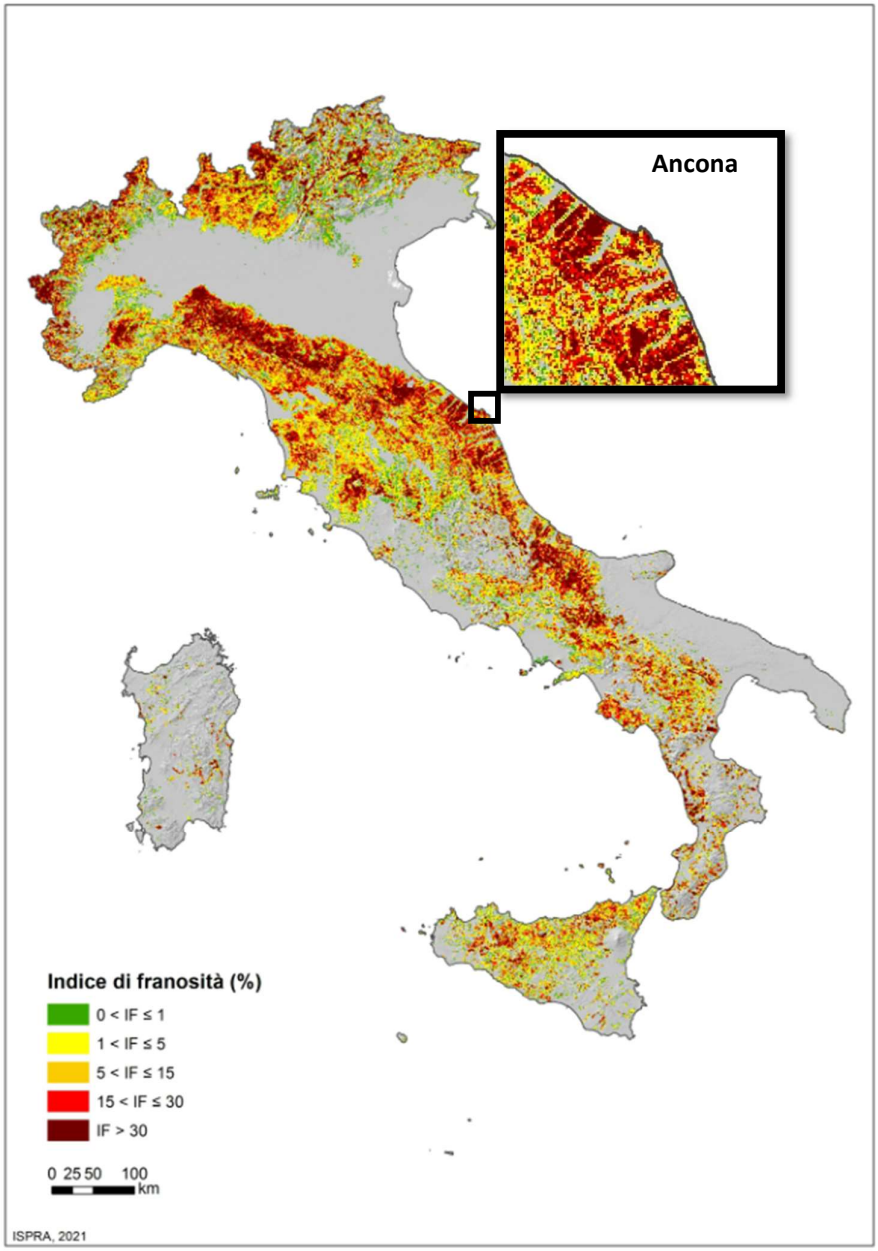

Figure 1 - Landslides Index (ISPRA).

2.2 Geological and geomechanical studies related to the area of interest and the nearby areas

Colosimo & Crescenti (1973) focused the attention to the need for geological and technical cartography to solve the problems of civil engineering with the aim of territorial conservation. In the technical map the stratigraphic units are distinguished and grouped according to lithological and geotechnical characteristics and the landslides are also reported.

Casagli et al. (1993) studied and, with a geomechanical characterization, the marly rocks of the Schlier geological formation (Fm.), which form most of the coastline near the town of Ancona. Are compared the strength properties of joints with laboratory data of weathered residual soils. Are analysed coastal landslides and all the phenomena involved in rock slope instability related to the poor quality of materials and weathering processes.

Iadanza et al. (2009) provided an account of the Italian framework regarding: a) the number, kinematic and distribution of coastal landslides; b) their state of activity; c) the most common damage and exposed elements; d) the mitigation measures. In Italy, more than 8,000 km of coasts consist of cliffs and rocky shores (about 35%), in which many villages and cities are located, some of them dating back to Roman or Greek times. The most frequent landslide kinematics are rock falls, slides and debris flows, leading to high risk in few areas.

Fruzzetti et al. (2011) gave us an analysis of the slope movements that have affected and affect Monte Conero. The promontory is presented according to the typical morphology of active cliffs characterized by a sinuous and jagged plano-altimetric trend. We therefore want to classify gravitational phenomena following an integrated and multidisciplinary approach with a prevalent geotechnical orientation, focusing attention on the role that the mechanical behavior of the rock types present, associated with the main morphogenetic processes, has and has had in relation to instability phenomena.

Aringoli et al. (2014) after a geological investigation of the area of the Coneto Mt., tried to define the probable geomorphological processes responsible for the genesis of the Conero which are identified in the activation of ancient and recent landslides, and to understand the most probable reasons that have prevented marine dynamics from eroding them.

Montanari et al. (2016) presented the problem of landslide instability in Italy describing the geology and morphology that characterize the Conero Mt. area, Ancona. They reported and analysed the case of the landslide of Portonovo, the beach at the foot of the Conero Mt.: 5 million m3 of rock collapsed from the mount down from 400 m elevation.

Pepi (2021) in his thesis work defined the main mechanisms of rupture that occur in the rocky wall of the Passetto (Ancona) trying also to understand the role that precipitation has on them. The mechanism of infiltration into the soil and the characteristics of the fracture system of the site were studied. A detailed analysis of fracturing was conducted using the scanline method and Discrete Fracture Network Modelling. The entire study was possible through a multi-level approach in which hydrogeology and geomechanics were involved. In particular, cumulative precipitation data were analysed by coupling this information with landslide phenomena (documented in the area). The rate of surface soil infiltration was determined using a double-ring infiltration test. The latter analysis was conducted together with tracer testing to understand the role of fracturing on groundwater circulation in the rock mass.

2.3 Remote sensing techniques applied to rock mass characterization

Sturzenegger et al. (2009), revised the application of terrestrial digital photogrammetry and laser scanning for the investigation of a rock mass in terms of fracture system. Frequently, remote sensing techniques are combined with traditional methods such as scanline to provide more information about an outcrop, allowing studies even in inaccessible and unsafe areas.

Pitts et al. (2017) integrated traditional field methods with the new digital techniques trying to analyse deep-water and channel-fill deposits. With this multi-level approach, he tried to collect informations and characterize a turbidite channel-lobe system of the Gorgoglione Flysch formation in Southern Italy. This innovating combined approach improved the data collection and the outcrop characterization.

Loiotine et al. (2019) explored rock mass characterization methods combining traditional field surveys with remote sensing techniques. In practice, traditional survey methods are particularly difficult and sometimes dangerous in steep and inaccessible areas. As a result, there is a risk of making sampling errors and often the data collected are not sufficient for a complete geostructural and geomechanical characterization of the outcrops. At this scope remote sensing techniques are used: digital photogrammetry technologies, Terrestrial Laser Scanning (TLS), LiDAR (Light Detection and Ranging) and Unmanned Aerial Vehicles (UAVs).

James et al. (2019) showed some guidelines on the use of photogrammetry in geological investigations and characterizations, increasing the number of information, in particular images, especially from unmanned aerial vehicles.

Devoto et al. (2020) tried to demonstrate the benefits of using drones to survey a large and slow-moving landslide along Malta's northwest coast. Particular attention was paid to the analysis of gravitational fractures and megacrust deposits at four study sites chosen for the presence of prominent examples of lateral spread developing into rocks. Google Earth (GE) image analysis and unmanned aerial vehicle (UAV-DP) digital photogrammetry are used in this study.

Francioni et al. (2020) showed how the use of unmanned aerial vehicles on inaccessible steep slopes is critical to define fracture intensity, block volumes and rockfall trajectory. They presented a new approach to define block volume distribution in rockfall simulations using an unmanned aerial vehicle (UAV): they tried to create a 3D model of the area to better define data obtained from conventional geomechanical surveys and to identify significant changes in the fracture intensity.

Jablonska et al. (2021) investigated a large discordant breccia body in the Puglia marginal basal carbonate formation in order to analysing and interpreting the behaviour of seismic cliffs. In order to study those inaccessible and unsafe areas, the investigation and data collection were carried out through UAV system.

He et al. (2021) wrote about maximizing impacts of remote sensing surveys in slope stability. Their work proposes a new method to predict landslide using GIS-based kinematic analysis. Discontinuities, detected from photogrammetric and aerial LiDAR surveys, were included in the assessment of potential rock slope instability through GIS.

Schilirò et al. (2022) described an integrated approach to investigate rockfall events from drone and satellite-based data in the Sorrento Peninsula, southern Italy. In this research they used a combined approach that integrates different remote sensing data and techniques. In particular, geostructural information about rock masses were generated through the geological interpretation of virtual outcrop models (VOMs).

Mammoliti et al. (2022) tried to evaluate the fracture system of the rock mass, evaluating all the geo mechanical properties of an outcrop located in an inaccessible area where the classical geological survey methods would be difficult and unsafe. They demonstrate that the remote sensing techniques were the best options for the analysis.

2.4 Discrete Fracture Networks (DFNs)

Maffucci et al. (2015) tried to perform an analysis of the Cretaceous sandstone reservoir of Rosario de La Frontera defining the fracture system of this site and trying to model it. They built a discrete fracture network (DFN) in order to characterize the fracture system and all its properties for geothermal investigation.

Karatalov et al. (2017) performed an analysis over 200 Discrete Fracture Network models (DFN) with varying input parameters to quantify the impact of the input variables in natural fractured reservoir characterization and modelling. The product can help reservoir characterization by identifying the main flow controls and by assessing the range of possible outcomes. The results led to the classification of three most critical parameters: fracture aperture, scale-up algorithm, and fracture intensity. These three have a significantly higher importance on all the other, except for the length that can influence in a minor way the results.

Lei et al. (2017) presented a discussion on the use of discrete fracture networks (DFNs). They highlighted the complexity in the study of fractures within a rock system and the difficulty in defining all the properties and behaviours: geometrical characteristics, geomechanical evolution and hydromechanical behaviour. Then they tried to fix the main steps for the creation of a discrete fracture network as true to reality as possible.

Massaro et al. (2019) studied the Triassic Jurassic reservoir units of the NW Lurestan region, Iran. They performed this study elaborating a discrete fracture network (DFN) of the fracture systems characterising the analysed succession. The data obtained by the DFN have allowed a more detailed analysis of the distribution and movement of flows within the system: in particular the relative connectivity and relative properties have been defined.

Volatili et al. (2019) studied the Roman Valley quarry (Majella Mountain, central Italy), well-known for the bitumen extraction. Combining laboratory tests and DFN modelling, they focused on how the role of stratigraphy and different structural features of the carbonate reservoir influence the distribution and movement of the fluid inside the system.

Tuckey (2022) investigated a case study in a coastal cliffs and wave-cut platforms near Sydney, Australia, using UAV photogrammetry mapping and creating a discrete fracture network with the aim of characterize the geomechanical properties of the rock masses. Is presented a workflow for UAV photogrammetry survey, discontinuity mapping, simulation of rock mass scale laboratory tests, and 3D DFN simulations.

3. Geological setting of the Umbria-Marche Domain

The Umbria-Marche succession (Figure 2) is a sequence of sedimentary rocks formed in central Italy from 220 million years ago (Jurassic period, Mesozoic era) until the Quaternary era.

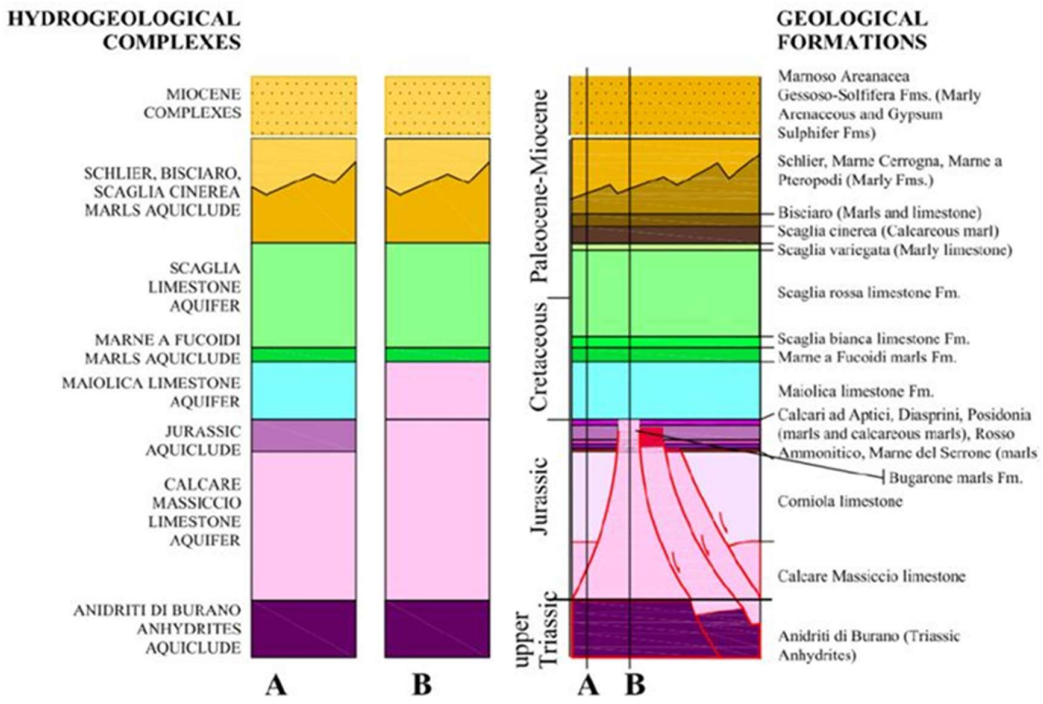

Figure 2 - Hydrogeological complexes and geological formations of the Umbrian-Marche domain.

The oldest rocks in the Umbria-Marche Apennines belong to the Upper Triassic (220Ma) and are represented by the Evaporiti and Dolomiti (Anidriti of Burano).

The stratigraphic sequence continues with the Calcare Massiccio, consisting of whitish gray micritical limestones, corresponding to a low water platform environment, generally arranged with a massive appearance.

During the Lower Jurassic, the transtensional oblique and transversal fault systems was responsible for the carbonate platform disarticulation in different domains. The Jurassic tectonic displacements give rise to horst and graben structure characterising a different sedimentation respectively defined to as complete, condensed, and lacunose, accordingly to the deposition environments.

In particular, we can distinguish: Corniola (200m thick), consisting of micritical limestone, of pelagic environment, gray-havana color with clear and regular stratification; Marne di M. Serrone (up to 150m thick), calcarenites and marly calcilutites that, upwards, pass to marl and reddish clays and flaps of Rosso Ammonitico (40m thick), partially heteropic with the Marne di M. Serrone, consisting

of reddish clay marl and marl (with carbonate intercalations) rich in fossils; Calcari a Posidonia (up to 200m thick), formation of pinkish micritical limestones, with marly component prevailing downwards; Calcari Diasprini (up to 150m thick) subtly layered marly limestone and limestone, gray-green, with polychrome flint.

In the following period, which goes from the Cretaceous to the Paleocene (145-22 Ma), the sedimentation continues with the Maiolica, a powerful limestone deposit ranging between 150 to 450 m thickness. Above the Maiolica we find the Marne a Fucoidi (50-80 m thick), consisting of marl and marly clays of various colors and, subordinate levels of limestone and marly limestone.

Belonging to the Late Cretaceous we find the formation of the Scaglia, which includes the powerful layered pile of limestone and/or limestone-marly and is divided into: Scaglia bianca, represented by whitish micritical limestones, well stratified, with intercalated levels of black flint (50-70 m) and Scaglia rossa represented by pink and red micritical limestone with intercalations of marl and flint, with thin and regular stratification (200-400 m).

Arriving at the late Eocene are deposited: la Scaglia variegata (50m thick), consisting of stratified marly and marl limestone, la Scaglia cinerea (200m thick), consisting of thinly stratified marly and marl limestones, with intercalations of leafy shales, gray or greenish-gray, the formation of the Bisciaro (50-150m thick) consisting of marl alternating with marly limestone of gray and greenish-gray color well stratified and the formation of the Schlier consisting of an alternation of clayey marl and marl and to a lesser extent of finely detrital whitish marly limestone.

The formations described so far constitute the backbone of the territory (bedrock) locally covered and /or masked by continental clastic deposits of the Plio-Pleistocene age.

From this period, the geological history of the Umbria-Marche domain passes from a predominantly marine to a continental environment. Dating back to the Pliocene and Pleistocene-Quaternary (5-1.65 Ma) we meet: marine deposits, colluvial deposits, that are frequent on most of the slopes and often fade into the surface alteration layer, eluvial deposits, present in large depressions or in small basins of prevalent karst nature, groundwater debris, present at the foot of the steeper slopes in layers of variable thickness, sometimes considerable.

4. Study Area

4.1 Geographical and geological framework of the study site

The study site is located on the coastal cliff of Ancona city (Marche Region, central Italy) (Figure 3), which extends for 15 km between Ancona city and Numana village.

The city, overlooking the Adriatic coast of the peninsula, stands on a promontory in the shape of a "bent elbow", protecting the harbor, that is one of the largest in Italy.

Figure 3 - Ancona top view (rivieradelconero.info).

The port docks are surrounded by the hills on which the historic districts are located: the Guasco hill with the Duomo, Monte Cappuccini with the lighthouse, Monte Cardeto, the Astagno hill with the Cittadella, and the hill of Santo Stefano with the Pincio.

The promontory divides the city in two areas, very different at a morphological level.

To the nord we find the Gulf of Ancona: the hills come close to the sea, but do not form cliffs; in this area there is the sandy beach of Palombina (Figure 4), bordered by the railway line.

Figure 4 - Palombina beach, north of Ancona (rivieradelconero.info).

Of a completely different nature is the area looking to the south of the Duomo hill which has a high and rocky coast and extends to Conero Mt., a relief of the Umbria-Marche Apennines, 572 m above sea level (Figure 5).

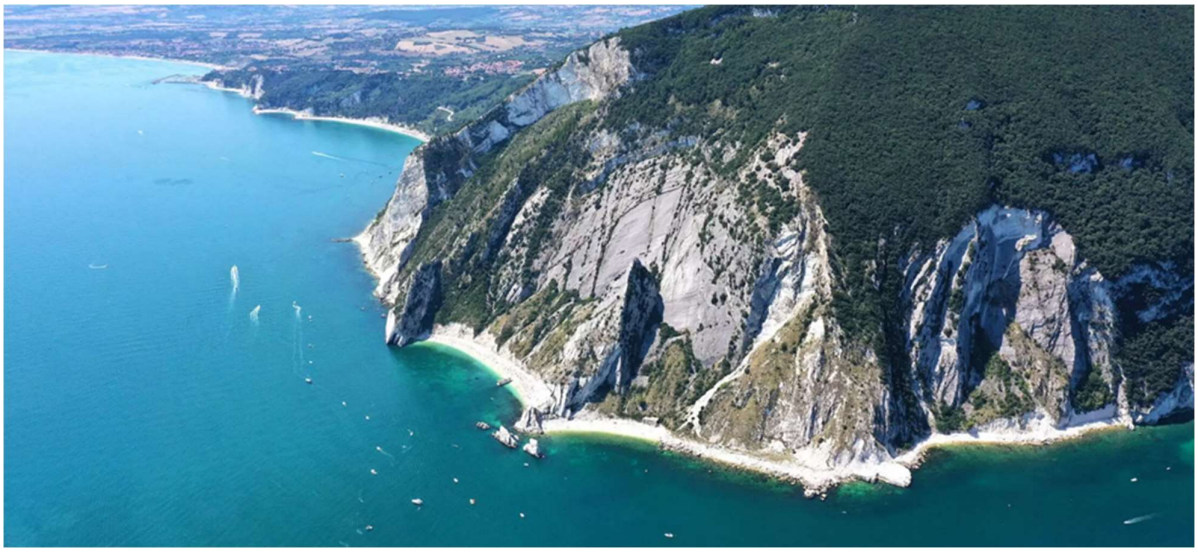

Figure 5 - Conero Mount, south of Ancona (lovelyAncona).

The Conero is the most important Italian promontory of the Adriatic, after that of the Gargano, and has the highest maritime cliffs of the entire eastern Adriatic coast: more than 500 meters overlooking the sea. The coast associated is called Riviera del Conero. Among the beaches of this stretch of coastline we remember the Passetto beach, the one investigated in this thesis, the beaches of Mezzavalle, Portonovo, and Le Due Sorelle beach (Figure 6).

Figure 6 - Most popular beaches in Ancona: a) Passetto b) Mezzavalle c) Portonovo d) Le Due Sorelle.

For its beauty and for the heterogeneity of the landscapes, the entire Conero area is a reference point for tourism, attracting thousands of tourists from all over Italy and Europe.

However, these areas are also known for erosion and instability, due to the morphology of the environment.

In coastal areas like this, powerful waves crashing against cliffs can erode the base, creating overhangs or unstable slopes. This erosion weakens the cliff structure and increases the landslides (Figure 7).

Also the slope, or gradient, of a cliff plays a significant role in determining the stability of the cliff; the force of gravity acting on the mass of soil and rock becomes stronger, making it easier for the material to overcome the friction holding it in place. Steep slopes can also experience more rapid erosion due to the increased velocity of water runoff.

It is important to note that landslides can have various triggers, and erosion and slope steepness are just two contributing factors. Other factors such as groundwater circulation, geological composition, vegetation cover, seismic activity, and human activities, can also influence landslide occurrences.

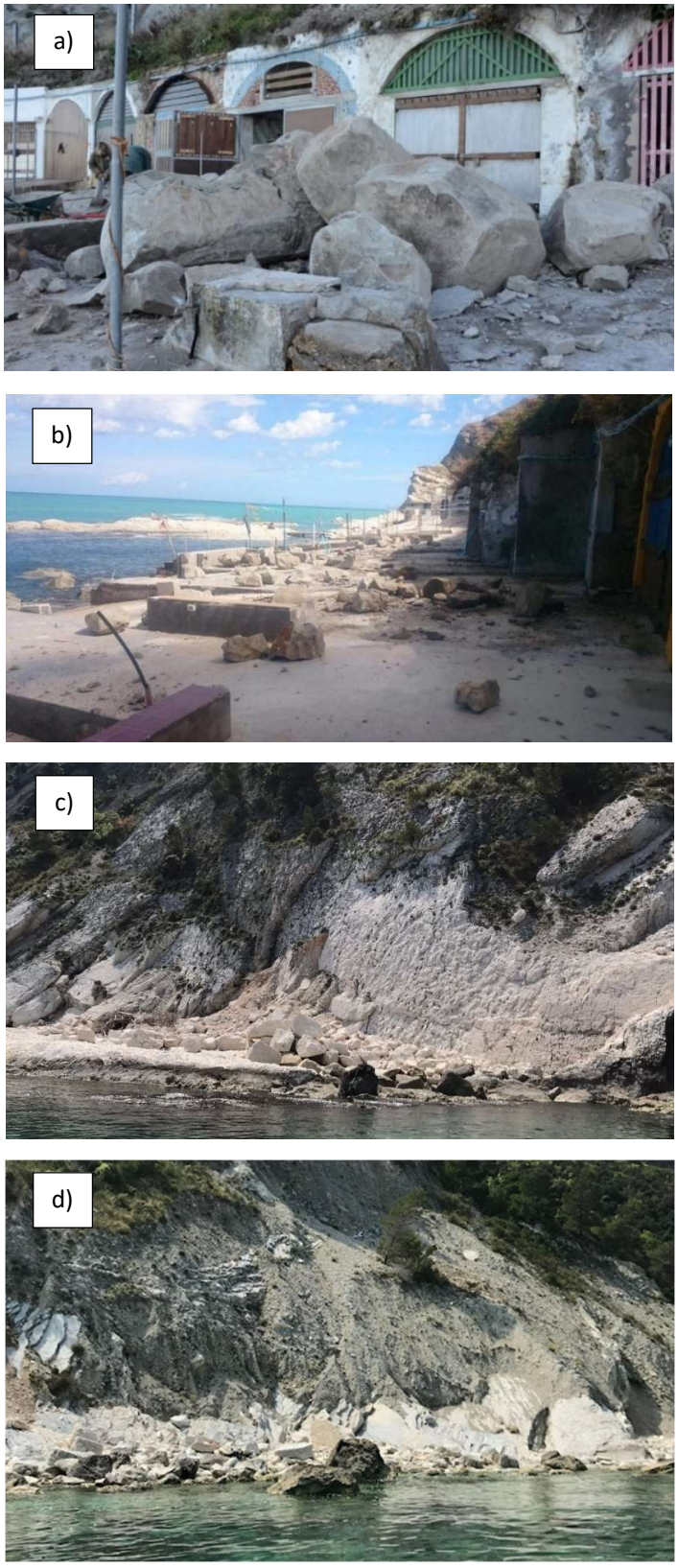

Figure 7 - Rock blocks fallen in Passetto area (Corriere Adriatico, Cronache Ancona) a), b); c), Landslides at La Vela beach c), d).

Therefore, considering all the activities present on the coast, it is very important to study and continuously monitor these critical areas.

The characterization of the Ancona area and Conero Mt. was done following the studies of Fruzzetti et al. (2011) and Aringoli et al. (2016).

The study area is characterized by steep cliffs with an average height usually higher than 100 m. It is composed mainly of marly-clayey formations of the Neogenic age and, only in the Conero Mt. massif, of Cretaceous-Paleogenic limestones. It is a typical high sea cliff subject to rock falls and other slope movements, favoured by wave undercutting and by the slope of the cliffs. From a tectonic point of view the Ancona area is characterized by faults and folds trending NE-SW, in the direction of the Apennine belt, cut by transverse tectonic lines. This structural pattern is the result of several tectonic phases during the Apennine orogenesis.

- Compressive phase of the middle Pliocene age, responsible for the major structures.
- Phase of subsidence, aged between the Upper Pliocene and the Basal Pleistocene, which reports marine sedimentation conditions.
- Phase of uplift that probably begins in the lower Pleistocene and which, with several events, leads to the emersion of the whole Ancona area.

The geological history caused the formation of subvertical high coastal cliffs, with morphological discontinuities and saddles. We can distinguish different lithostratigraphic units based on the geological map of the site (Figure 8):

- The Maiolica Fm, the Marne a Fucoidi Fm. and the Scaglia Bianca Fm., which belong to the Cretaceous chronostratigraphic unit. The Scaglia Rossa Fm. (Eocene). The Scaglia Cinerea Fm. (Oligocene).
- The Bisciaro Fm. and the Schlier Fm. (Miocene).
- The Marls of Monte dei Corvi Fm. (Miocene-early Pliocene).
- The Marls of Numana Fm. (late Pliocene).
- Recent continental deposits to the Quaternary.

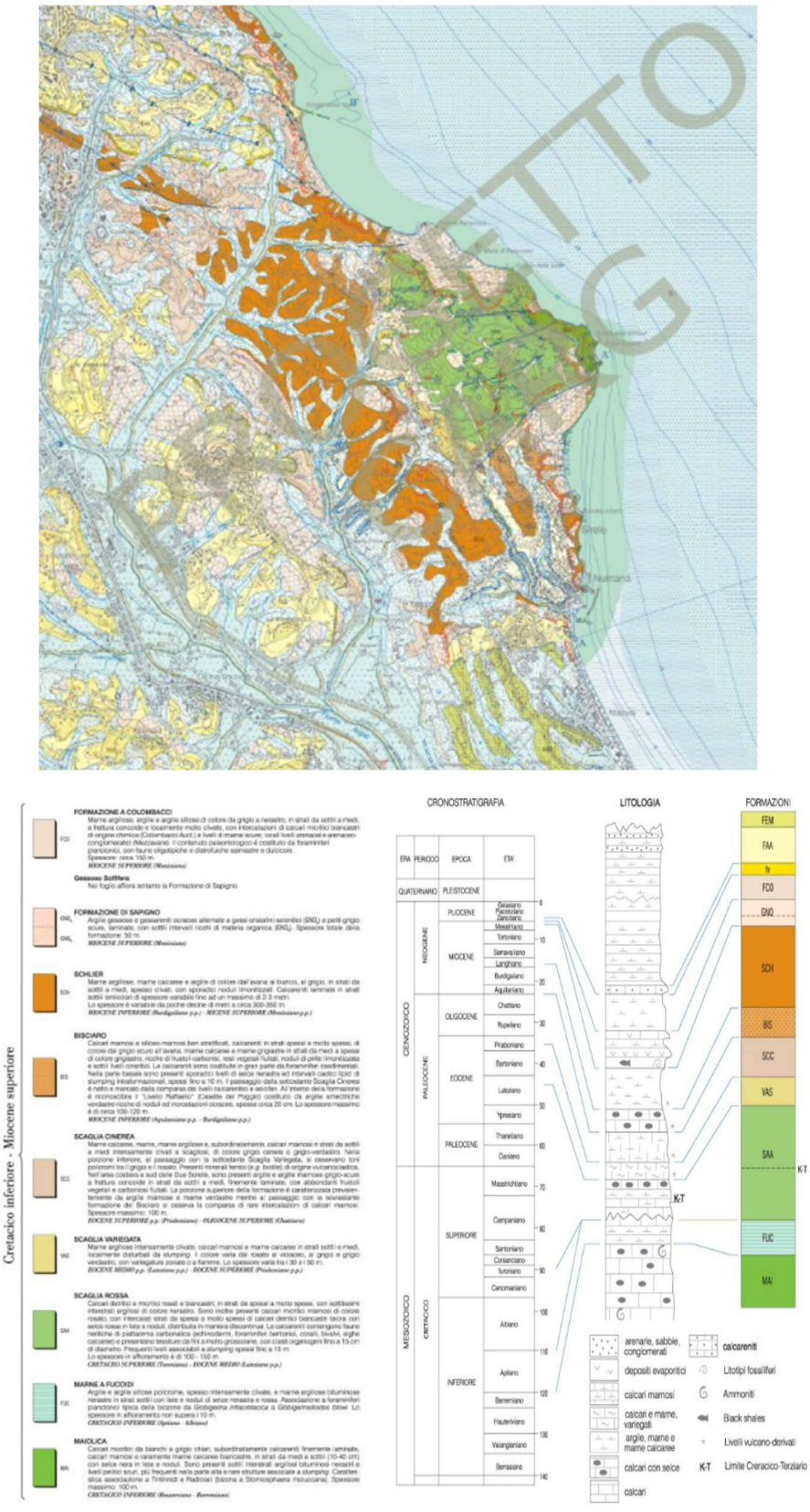

Figure 8 - Geological map of the site (isprambiente.gov.it).

The Maiolica (MAI) consists of white, hard, and compact limestone, which come in layers of 20-40cm, interspersed with levels of flint; the outcropping thickness is of the order of 100m. This formation has very good mechanical characteristics: about 100 MPa of Uniaxial Compressive Strength value (UCS).

The Scaglia Bianca (sb) and the Scaglia Rossa (sr) are stratified limestones, also of good mechanical characteristics: UCS = 75-90 MPa for sb, slightly lower characteristics for sr when the marly component increases and limescale levels become thinner especially in the upper part of the unit.

Interposed between these units with lithoid behavior, we find the geological formation of the Marne a Fucoidi (mf), whose geotechnical properties depend both on the degree of fracturing and on the degree of alteration. The mf, subtly stratified, easily degrades into flakes of various sizes manifesting a behavior closer to that of a land than a rock. The presence of these bituminous marls is due to a period (30 million years ago) of tectonic quiescence and stagnant sea that favored the deposit of calcareous mud rich in planktonic microorganisms; the Fucoidi, which give the name to the unit, are organisms of which fossil traces have been found.

The Scaglia Cinerea (sc) is represented by marly and marl limestones thinly stratified with marly component that increases upwards of unity; this formation, in relation to the tectonic deformation degree and alteration, passes from soft rock (UCS = 20-25 MPa) to that of a granular material. The alteration produces fine material that can be classified as a "Low Plasticity Silt" (ML).

The Schlier (sh) includes grey and white marl limestone, marl and clay marl; the amounts of calcium carbonate decrease from the bottom to the top of the unit. Also in this case, when you are sheltered from exogenous agents, the behavior is that of a massive stone rock (UCS = 15-23 MPa), but when the tectonic disturbance and degradation are high, the mechanical behavior of the cluster is dominated by the fine matrix that is generated, classifiable as "Silt or Clay of high plasticity" (CH-MH).

The Marne of Monte dei Corvi (mC) are marls and marly clays.

The Marne of Numana (mN) are also part of the over consolidated Pliocene clays widespread in the foothills of the Middle Adriatic. Those of Numana are strongly tectonicized, emerge only in the southern part of the examined area, are classifiable as silty clays with levels of fine sand of low plasticity.

Following the work of Aringoli et al. (2014), based on the lithologies outcropping, the Ancona coast near the Conero Mt. can be subdivided into four different zones (Figure 9), to identify the type of instability events mainly occurring:

a) Cardeto park: this area is characterised by predominantly pelitic terrigenous lithotypes, such as the marly-silty clays of the Schlier Fm. (Upper Miocene), the Colombacci Fm. given by clayey marls with conglomeratic levels (Upper Miocene), the characteristic Orizzonte del Trave Fm., that is a strongly cemented arenaceous-calcarenite level (Upper Miocene) and the pelitic and pelitic-sandy lithofacies of the Lower Pliocene. This area is mainly interested by erosion and frequent landslides that always reach the shoreline to be then dismantled during the most intense storms.

b) From Portonovo to the Scoglio della Vela: In Portonovo the cliff has an average height ranging from 350 and 420 m, where the most outcropping formation is the Scaglia Rossa Fm., belonging to the north-eastern flank of an accentuated and asymmetrical anticlinal fold. The coast has considerably inclined layers, mostly according to an oblique dip-slope. The core of this fault is constituted by the oldest lime formation, the Maiolica. The main events here are individuated in sliding flow and rock fall between the Church of Santa Chiara Maria and Scoglio della Vela (Figure 7).

c) The area between the Scoglio della Vela and the rocks of the Due Sorelle: this area shows very high slopes and differences in height; the lithostratigraphic units of the Scaglia Bianca, Scaglia Rossa and Maiolica Fms. outcrop. The strongly inclined layers characterise the cliff, with average immersion towards the sea, forming the north-eastern side of the anticlinal fold. In this stretch of coast, extended phenomena of rock fall and translational sliding can be observed.

d) The southern part comprehending the beach of San Michele in Sirolo: is the less steep area of the cliff, due to the high erodibility of the calcareous marls of the Scaglia Cinerea Fm., although in the upper part and towards Sirolo there are calcareous-marly and marly outcrops of the Bisciaro and Schlier formations.

Figure 9 - Lithological division of the area: a) green line b) orange line c) blue line d) red line (Google Earth).

4.2 The Passetto sea cliff

After briefly presenting the area of Ancona, with its various morphological and geological facets, we are now going to frame and describe the area of interest of our work, the Passetto sea cliff (Figure 10).

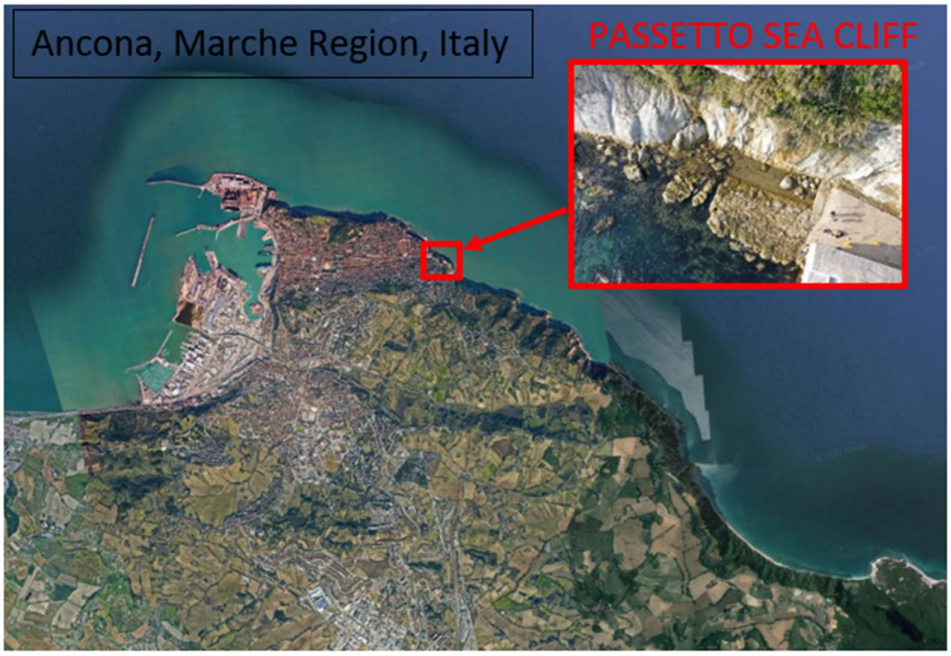

Figure 10 - Passetto sea cliff frame (Google Earth + UAV photo).

Already mentioned above, the Passetto is one of the most popular areas that characterize the city. The beach, rocky, is located at the end of Viale della Vittoria, in the Adriatic district, where the pine forest area overlooks the sea. From the “Monumento ai caduti” you go down a large white staircase and arrive directly at the beach (Figure 11). Once you get off, continuing on the right and passing the restaurant "La Luna", you arrive at the area of interest.

Figure 11 - Passetto sea cliff, Monumento ai caduti.

The geological formation mainly studied in this thesis is the Schlier (Figure 12).

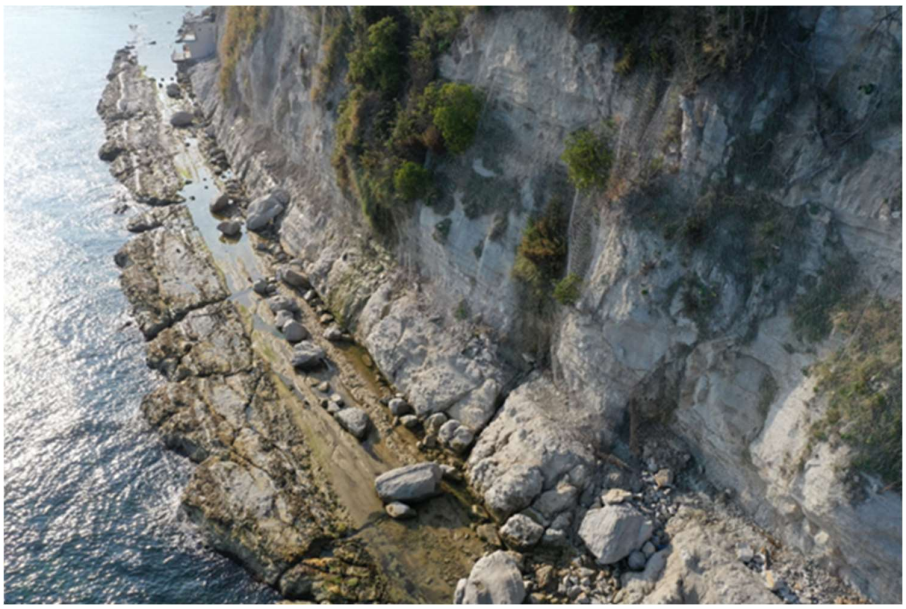

Figure 12 - Schlier geological formation (Passetto sea cliff).

The schlier represents one of the most widespread and extensive formations of the Umbria-Marche Apennine (Dubbini et al., 1991; Casagli et al., 1993). In the literature a real type of section has not been indicated, but different sequences have been analyse that can represent a reference for the different sectors of the Umbria-Marche Apennines: Gubbio-La Contessa, Sant'Angelo in Vado, Visso for the inland areas, Ancona for the external areas.

This stratigraphic unit owes its name to the contemporaries and similar deposits, from the lithological point of view, that are found in Austria within the Vienna basin.

It is considered a hemipelagic formation (environment where only the finest materials from the continent are deposited) and its thickness is very variable from area to area. This is due both to the variation of morphology of the seabed in which the formation is deposited, and due to heteropic variations (lateral variations of facies for which sediments, although deposited in the same time interval, have different characters according to the specific palaeogeographical conditions of the sedimentation basin) with other Miocene formations (for example the Marls with Cerrogna in the southern sector of the Region).

Indicatively, thicknesses can be indicated ranging between 50 and 300 m.

As far as the age of formation is concerned, this tends to become gradually younger moving from west to east, in accordance with the phases of structuring of the Apennine chain and the migration of

the chain system during the Miocene. An age can be indicated between the upper Burdigalian – upper Langhian, in the westernmost areas, to the basal Messinian in the easternmost areas.

From the lithological point of view, it consists of an alternation of marl and clayey marl and to a lesser extent of finely detrital whitish marly limestone. The clay content tends to increase towards the top of the formation. The color is whitish in the lower and middle part of the complex, predominantly grayish in the upper one. The stratification is not very clear and generally stands out only for the greater calcareous content of some layers which, due to the greater hardness, appear more protruding than the less resistant layers. The layers are generally medium-thin, and the bioturbation (action of living organisms in the sediment) is quite intense. Lithoid elements tend to break with "conchoid fracture" (i.e., curved surface). In case of intense tectonics, fracture systems can be produced so dense as to reduce the marl into minute elements that tend to give rise to thick layers of debris at the foot of the outcrops. Marly abounds in fossil shells of planktonic foraminifera, which can be observed with a magnifying glass or directly with the naked eye.

Within the Schlier are also found thin volcanoclastic levels, very altered, with the typical rust color due to the presence of iron oxides and hydroxides that derive from the diagenetic transformation of volcanic glass. Given their lower competence to atmospheric agents (exogenous agents), deep and characteristic erosion grooves can be formed at these levels, which tend to highlight the marly-calcareous layers within which they are contained. In the upper part of the unit there is a characteristic horizon of smectic clays, a clayey mineral composed mainly of montmorillonite, (improperly called Bentonite), which can reach up to one meter thick.

As mentioned above, the Umbrian-Marche Schlier is characterized by a strong variability with regard to thicknesses, lithofacies and age. In the external areas of the Umbria-Marche Apennines (Ancona area) the Schlier is mainly characterized by an alternation of the following litofacies:

Litofacies a: characterized by gray-blue clay marl and marl (bluish green on the fresh cut). Its thickness varies from 20 cm up to 4 m.

Litofacies b: yellowish-white calcareous marl and marl (bluish-green when freshly cut) with a thickness of 20 to 40 cm.

Litofacies c: calcareous marl and yellowish-white marly limestone (greenish-gray when freshly cut).

The Ancona section (Figure 13) is certainly the most complete stratigraphic column, which can represent a reference section of the external Marche basin.

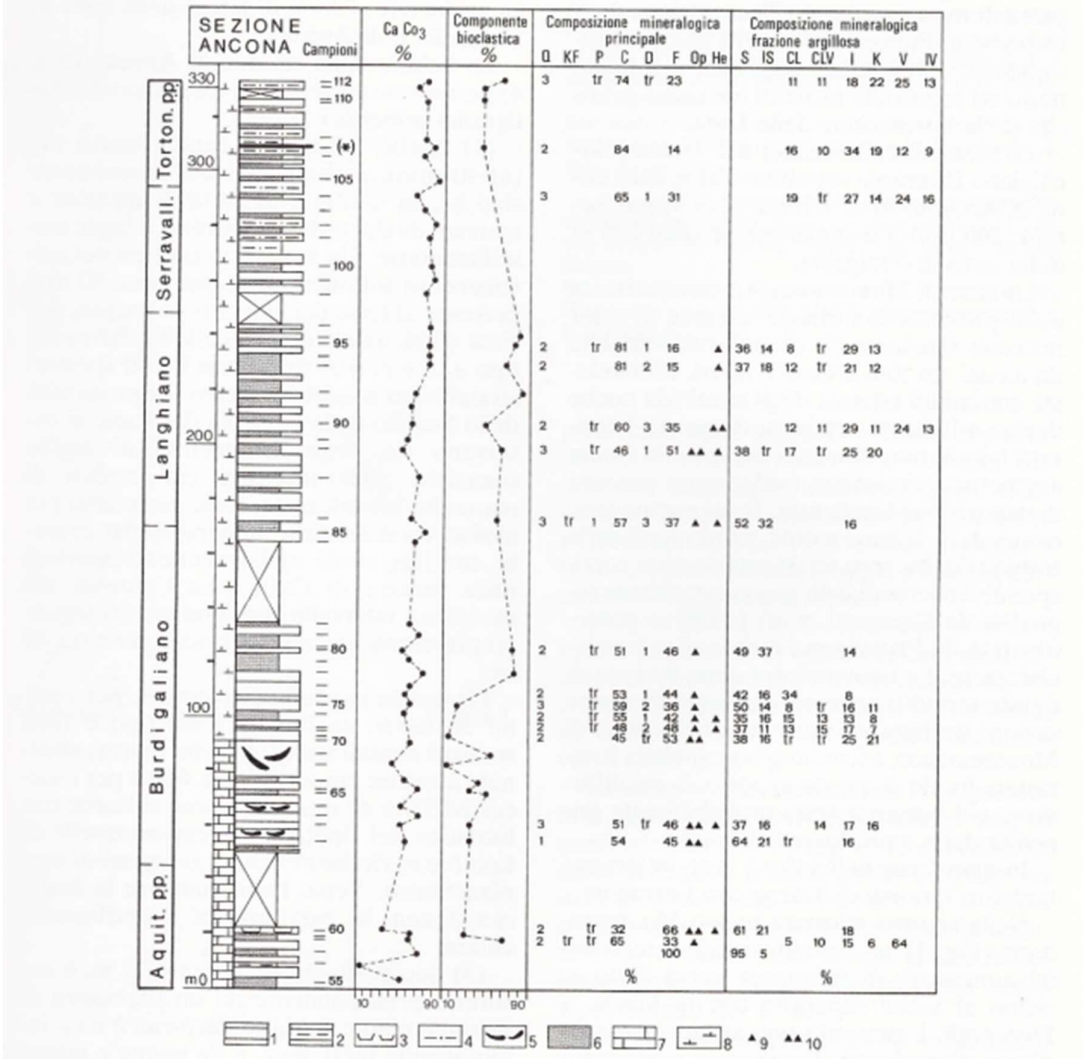

Fig. 4 - Litostratigrafia, composizione mineralogica semiquantitativa (principale e frazione argillosa), percentuale della componente bioclastica e del $CaCo_3$ della Sezione di Ancona.
1, marne, marne calcaree e calcari marnosi (*litofacies b* e *c*); **2**, argille smectiche; **3**, marne tripolacee; **4**, argille marnose, marne e marne calcaree tutte bituminose (*litofacies f*); **5**, intervalli slumpizzati; **6**, marne e marne argillose (*litofacies a*); **7**, Bisciaro; **8**, Schlier; **9**, presenza apprezzabile; **10**, presenza più che apprezzabile; **Q**, quarzo; **KF**, feldspato potassico; **P**, plagioclasi; **C**, calcite; **D**, dolomite; **F**, fillosilicati; **Op**, opale; **He**, heulandite; **S**, smectite; **IS**, illite-smectite; **CL**, clorite; **CLV**, clorite-vermiculite; **I**, illite; **K**, caolinite; **V**, vermiculite; **IV**, illite-vermiculite; **tr**, tracce.
(*) Livello ricco in biotite preliminarmente datato con radioisotopi con un'età di 11,1 + 0,3 Ma. (Montanari *et al.*, 1988).

Lithostratigraphy, half-quantitative mineralogical composition, $CaCO_3$ and bioclastic fraction rate per cent of the Ancona Section.
1, marls, calcareous marls and marly limestones (*lithofacies b* and *c*); **2**, smectitic clays; **3**, tripoli-like marls; **4**, marly clays, marls and calcareous marls all organic C-rich (*litofacies f*); **5**, slumping levels; **6**, marls and clay marls (*lithofacies a*); **7**, Bisciaro Fm.; **8**, Schlier Fm.; **9**, present; 10, common; **Q**, quartz; **KF**, K-feldspar; **P**, plagioclase; **C**, calcite; **D**, dolomite; **F**, phyllosilicates; **Op**, opal; **He**, heulandite; **S**, smectite; **IS**, illite-smectite; **CL**, chlorite; **CLV**, chlorite-vermiculite; **I**, illite; **K**, kaolinite; **V**, vermiculite; **IV**, illite-vermiculite; **tr**, traces.
(*) Biotite-rich level dated with a preliminary radioisotopic age of 11.1 + 0,3 Ma (Montanari *et al.*; 1988).

Figure 13 - Litostratigraphic and mineralogic composition of the Ancona section (Dubbini et al. 1991).

5. Materials and Methods

The working methods applied to this thesis are based on the combination of traditional geomechanical analysis using scanlines and photogrammetric remote sensing techniques using UAV (Unmanned Aerial Vehicle).

This multi-level approach has allowed to obtain a considerable amount of data and to carry out a statistical analysis of fracturing through 2D and 3D analysis that leads to the development of stochastic models of the fracturing of the rock mass (discrete fracture network, DFN).

For this purpose, the softwares Agisoft Metashape, QGIS with the NetworkGT tool and Move have been used.

5.1 Traditional geomechanical analysis - Scanline

The geomechanical survey was the first and fundamental approach to the investigation of the rock mass.

The conventional method provided by the standards is the scanline which consists of placing a tape on the outcrop of adequate length, i.e., extended at least 10 m or 10 times the mean estimated spacing.

The scanline methodology is a common technique used in rock mass investigation to gather information about the geological and structural characteristics of a rock mass.

First, the appropriate location and orientation of the scanline were determined; the scanline should pass through the areas of interest, such as zones of instability, high fractured zones, areas with different rock types.

Two different one-dimension scanlines, with length 11 m (Figure 14, blue line) and 8 m (Figure 14, red line) were performed. In order to collect more detailed data of sets of discontinuities we decided to make two different scanlines orthogonal to each other.

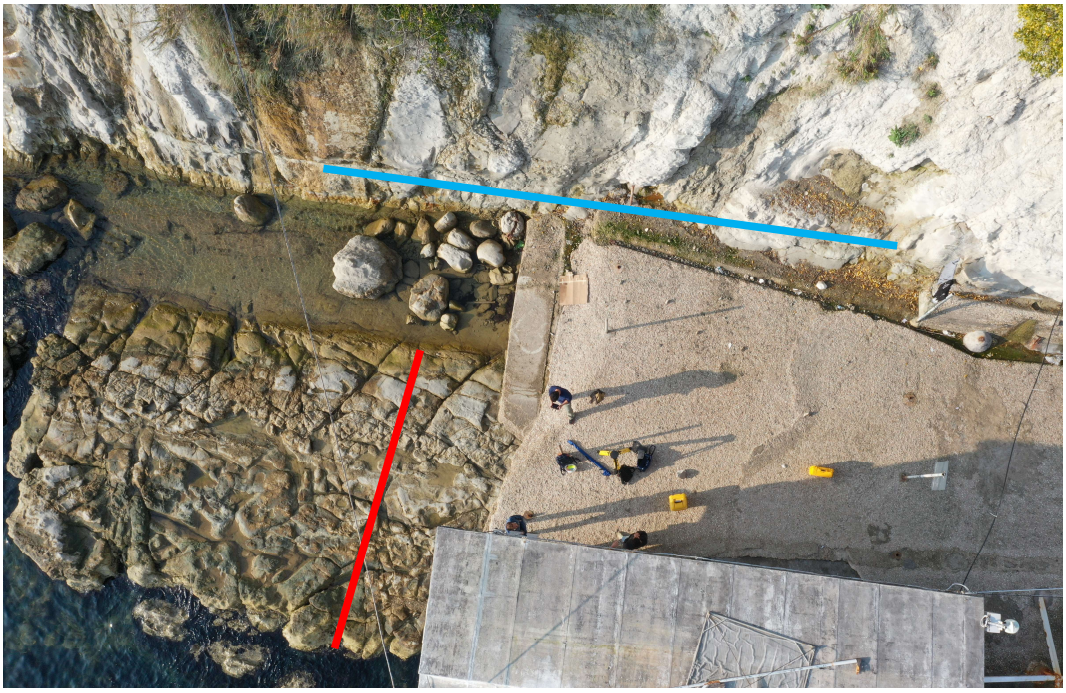

Figure 14 - Scanlines on the horizontal (red line) and vertical (blue line) portion of the cliff.

Walking along the scanline we visually inspected the exposed rock faces or outcrops looking for features such as fractures, joints, bedding planes, faults and weathering.

5.2 Unmanned Aerial Vehicle survey (UAV) – Drone

Nowadays, photogrammetry techniques, especially in the investigation and representation of the territory, play an important role. In traditional topography, the representation of the territory is achieved by detecting a series of characteristic points that are then returned analytically and drawn in the chosen scale (discrete relief or by points). However, the traditional topographic survey by points has some disadvantages: high costs for field operations, as the points must be recorded one by one, especially if the territory is of large extensions; need to associate to the measurements obtained from the goniometer also annotations that allow, in times after the measurement, to recognize the point to which they refer; need to perform interpolations both for the construction of contour lines and for the planimetric representation of nonlinear elements.

In 1839, with the invention of photography, it was decided to add the photographs to the traditional point relief. Thus, was born the idea of photogrammetry, which is a technique that helps to carry out survey operations with a camera instead of a goniometer. In this way the terrain, with its peculiarities

and its infinite points, becomes available for measurements and processing without requiring physical presence on the elements to be surveyed.

So, we can define photogrammetry as the technique that allows to define the position, shape and size of objects on the ground, using the information contained in appropriate photographic images of the same objects, taken from different points. (Cannarozzo, 2017)

First, to determine the positions of the points of an object in the real environment of the territory using the positions of the corresponding points on the photograph, it is necessary to define the geometric relationships between the three-dimensional positions of the points of the object and those of their images on the plane of photography (plate) (Figure 15). At each point of the three-dimensional object A, B, ... (object space) corresponds to a homologous point A', B', ... on the plate plane (image space). In this regard, it is possible, with sufficient approximation, to think of photography as a central perspective, according to which the segments that join the points of the object with their corresponding images (projecting star) all meet at a point O, a few centimeters away from the plane of the photographic emulsion (plate), called the center of taking.

The center of grip O is a point of the camera lens, while the distance of O from the plane of the plate is called the main distance and denoted by p. As we shall see, it remains fixed and can be considered (regardless of distortion) equal to the focal length of the same lens (p = f). The projection point of O on the plane of the plate is called the main point and is denoted by P, therefore PO = p.

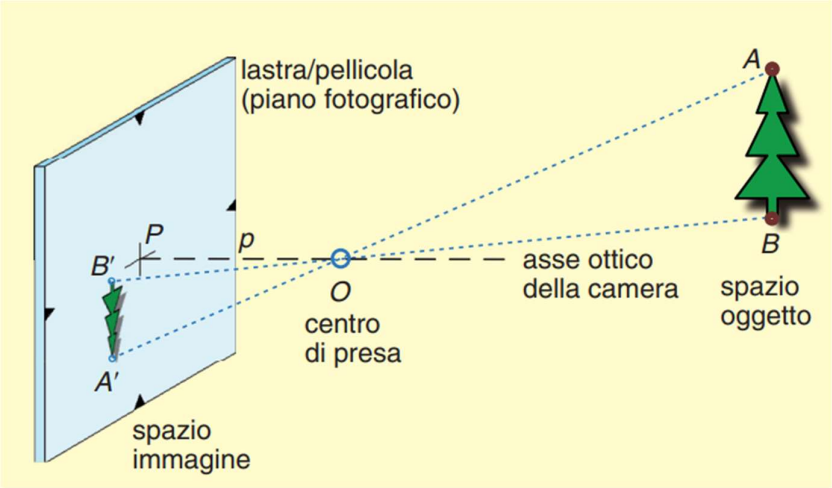

Figure 15 - Principle of photogrammetry technique (1) (Cannarozzo, Zanichelli, 2017).

A single photograph is not enough to define the position of the points on the ground (Figure 16). If you have two photographs that contain the same object from two gripping centers, its points are uniquely defined by the intersection of the homologous rays r1 and r2 (aerial grip configuration).

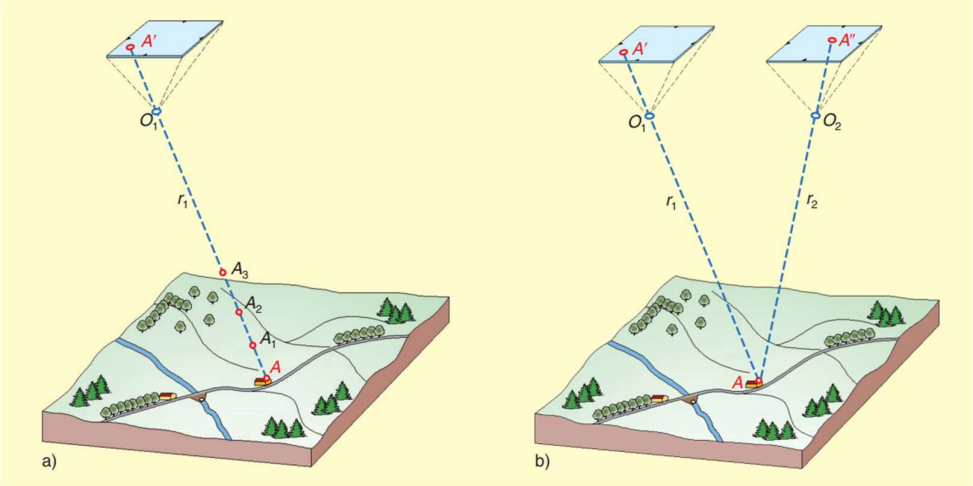

Figure 16 - Principle of photogrammetry technique (2) (Cannarozzo, Zanichelli, 2017).

In this context, point A of the terrain corresponds to the homologous point A'' on the first photograph and point A'' on the second photograph.

Precisely knowing the position of the homologous points A' and A" on the two photographs, and the spatial position of the two plates and the two outlet points O1 and O2, point A remains geometrically defined, as the point of intersection of the two projecting rays r1 and r2 that join the two homologous points with the corresponding gripping centers.

The positions of the O1 and O2 intake centers and the orientation of the plates, however, (with a few exceptions), are not known in advance.

However, it is possible to obtain this information from the photographs themselves, if they contain a certain number of points of support on the ground whose positions are obtained from traditional topographic operations (absolute orientation phase).

Today the photogrammetric problem is solved by obtaining the coordinates of the intersection in the space of the lines r1 and r2 with the resolution of a system of equations (called collinearity) obtained from analytic geometry relations (analytical photogrammetry), while in the past the same operations were carried out with analog mechanical (or optical) instruments, which allowed to establish the position of the generic point A within an object space reconstructed to scale reduced said model (analog photogrammetry).

In the photogrammetric survey the following phases are always recognized:

- Acquisition: operations concerning the taking of photographic images, carried out with appropriate cameras, called cameras, and appropriate techniques.

- Orientation: preliminary operations for the determination of the parameters that allow to position the gripping centers and the plates with the same position in the space they had at the time of the taking, then the reconstruction of the shape and size of the object taken.
- Restitution: operations that allow you to make measurements on the model of the reconstructed object, using tools called restitutors, able to produce, as a result, a drawing, a numerical set of coordinates or a straightened image.

Photogrammetry is then classified according to the type of socket used, to the type of processing, and to the type of photograph used.

Type of socket

- Terrestrial photogrammetry. The sockets are made from the ground; in this case the objects are located at distances of less than 200 m; so, we also speak of photogrammetry of neighbors (survey of buildings).

- Aerial photogrammetry. The sockets are made from an airplane; in this case the ground is located at distances greater than 200 m; so, we also speak of photogrammetry of the distant (relief of the territory).

Type of processing

- Analog photogrammetry. The reconstruction of the detected objects is obtained with physical devices (metal rods, light rays) that reproduce the phenomenon of the grip in reverse.

- Analytical photogrammetry. The reconstruction of the detected objects is obtained by numerically processing (with modern calculation tools) appropriate measurements made directly on the frames.

Type of photograph

- Classical photogrammetry. The photographs are obtained from the development of photosensitive emulsions on film, or on glass sheets (negative and positive).

- Digital photogrammetry. The photographs are obtained in numerical form and organized in a grid of pixels. They can be obtained either by a digital camera or by scanning a traditional photograph.

Photogrammetry with drone is one of the most advanced technological innovations of recent years in this sector and it is the one used in this work.

The photogrammetric aerial survey, as already explained, has existed for a long time, but the surveys with drones have opened new scenarios, making possible to get very close to the subject.

Drone photogrammetry allows access to hard-to-reach or inaccessible areas, providing detailed images faster than standard methods and at a lower price.

Photogrammetry using the drone or "aerophotogrammetry", has various technical applications: orthophotos, geological surveys, topographic services with drone, 3D models (point cloud reconstructions, contour lines), mapping of construction sites and territories, rendering buildings, monitoring sites with hydrogeological instability, DEM (Digital Elevation Model).

Thanks to this technique we were able to obtain information starting from the processing of several photographs taken from different points of view, to recreate the size, position and orientation of the object in question.

Once the photos were acquired, they were processed into a software, Agisoft Metashape, for the creation of a 3D model of the cliff.

A Mavic 2 Pro drone was used to investigate the sea cliff (Figure 17).

Figure 17 - Mavic 2 Pro drone.

It presents the following camera characteristics:

- 20-megapixel camera resolution.
- 28 mm focal length with f/2.8 to f/11 aperture.
- maximum image size of 5472 × 3648 px.

We operated the UAV flight (Figure 18) with the manual mode because the acquisition of the images was done very close to the cliff. To create a 3D model with a high resolution the UAV photographs were taken from an average distance of 20–30 m from outcrops.

Figure 18 - Mavic 2 Pro drone flights: acquisition of the cliff surface.

The acquisition of photograph was done in two different ways: for the subvertical cliff were done multiple vertical photographic strips while for the toe of the cliff were done oblique and nadiral photographs. In both cases, the side and frontal overlap was kept at about 70–80% and a total of 400 photographs were acquired, covering the entire cliff.

5.3 Total Station and Ground Control Points

Ground Control Points (GCPs), necessary for the orientation of photographs and the creation of the 3D model, were measured though a Trimble S7 Total Station (Figure 19).

Figure 19 - Trimble S7 Total Station.

The total station is a topographical instrument that is used for indirect topographic survey: the measurements are not directly acquired from the object but extracted from the result of different processes and calculation.

In the past, before the advent of total station, the angles were measured through the optical theodolite. However this technique did not allow the measurement of distances, creating some difficulties in mapping kilometers long stretches.

Then, to compensate this fault and improve performances in measuring distances of objects, was invented the electronic distance meter.

Finally, the combination of the two technologies for a complete and more detailed measurement, led to the creation of the Total Station: measurement of angles, oblique distances and gradients, were obtained from a single instrument.

The total station consists of:

- Base with the three lowering screws used to make horizontal the rotation plane of the station.
- Spherical level, used to approximate the horizontality of the plane.
- Telescope with distance meter: the telescope with viewfinder allows you to point objects while the electronic distance meter is responsible for measuring the distance between the instrument and the framed point.
- Electronic goniometer: the total station reads the horizontal and vertical angles through a graduated circle measuring the azimuthal angle and the zenithal angle.
- On-board computer: this is a control panel that allows you to enter survey data and immediately see the results.
- Tripod, important to stabilize the instrument.

To correctly start a survey with the total station, it is essential to correctly perform the stationing phase.

The stationing determines the correct measurement of the points and consists in positioning the station on the vertical of a materialized point, usually a fixed point, and then hooking it to the tripod with a screw. Meanwhile, the tripod legs must be well fixed in the ground to begin the relief phase.

The total station together with the laser plumb are switched on and it is checked if the instrument is plumb: for a correct stationing this red laser must center the stationing nail while the instrument is leveled. After this verification it is possible to perform the reset operation: that is, configure the zero angle on a reference (another nail or point).

At this point the total station is ready, and the positions and measurements can be acquired: for a correct measurement it is necessary to center each point with the telescope on the intersection of the lines that correspond to the optical center of the objective. The measurement considers vertical angles, horizontal angles and inclined distance and can be exported from the station in Polar coordinates or Cartesian coordinates.

The surveys with the total station are called celerimetric surveys, they are applied to the terrain and allow to overcome the difficulties of topographic survey in its classic version.

In fact, through the celerimetric survey it is possible to obtain plano-altimetric information through the speed measurement (in talian “celerimensura”), a topographic technique that, thanks to optical instruments and mathematical models, allow to reduce manual operations on the ground.

Once you have finished the topographic survey and determined the exact coordinates of all the points with respect to a Cartesian reference axis (X, Y, Z), you can transfer this information to your PC to process the recorded data.

Thanks to the total station we were able to identify our Ground control points.

Ground Control Points (GCPs) are points that are used to connect the photogrammetric survey to the actual size and orientation. This is the step to be taken to bring the images detected with the drone to have reliability in geometric terms. The main characteristic of a topographic survey is in fact that it is measurable.

In the operational reality of the survey, the GPCs are made visible by chromatic contrast markers (highly recognizable objects).

Through a special instrumentation (total station, GPS rod, other topographic instruments) the coordinates of the GCP control point identified by the marker are detected. These tools allow you to identify the location of the point with great accuracy.

However, a consideration must be made: an exact measurement of the coordinates of the point is useful only when the point on the ground is easily identifiable.

For example if from the photographs that are taken by the drone's camera it will not be possible to identify an exact point, then the precision used in detecting the coordinates cannot be translated into geometric accuracy of the model.

More precisely, as GCPs, were chosen those natural features, like fractures or objects, easily visible on the outcrop and on the images acquired by the drone. A total of eighteen GCPs were measured.

For the acquisition of these GCPs, some have been chosen and marked easily where possible (Figure 20), others, in areas impossible to reach, have been taken considering clearly visible reference points (Figure 21) thus managing to trace the entire area of interest.

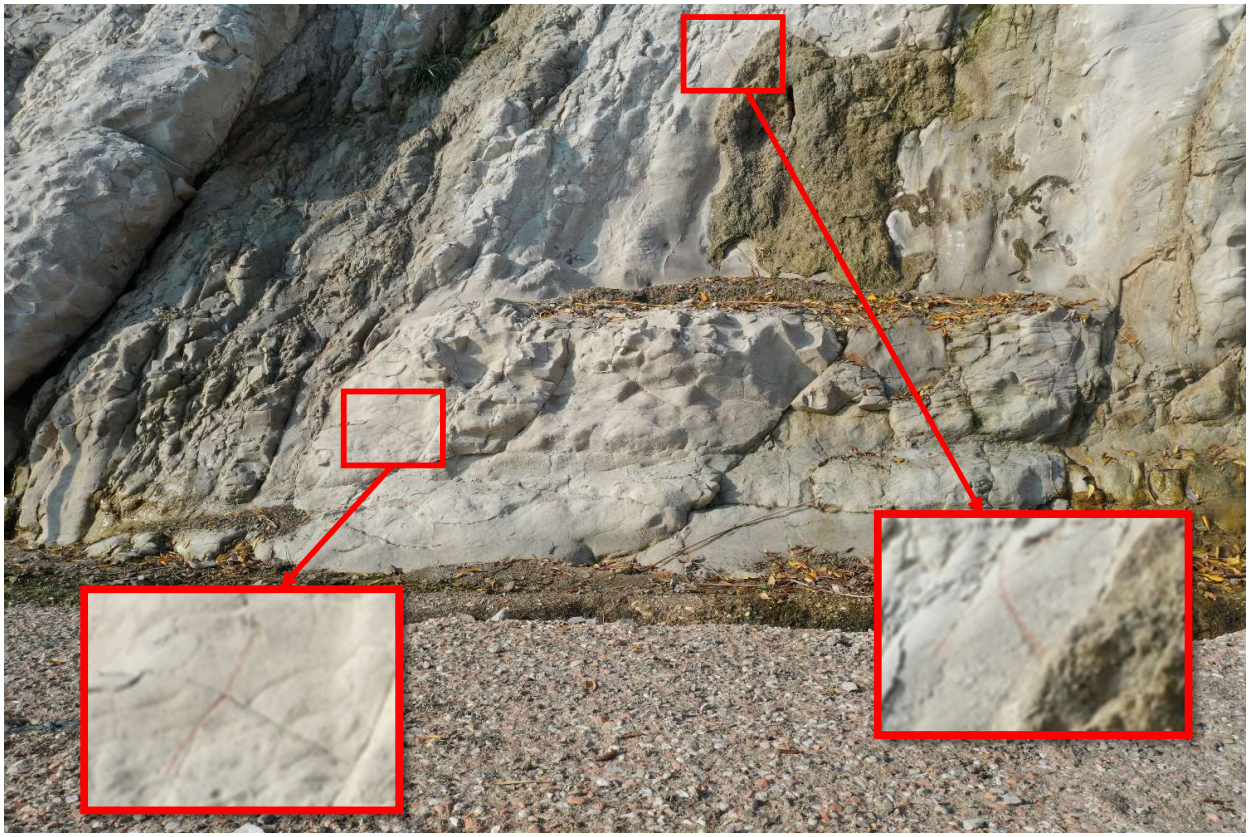

Figure 20 - Ground Control Points (GCPs) easily marked.

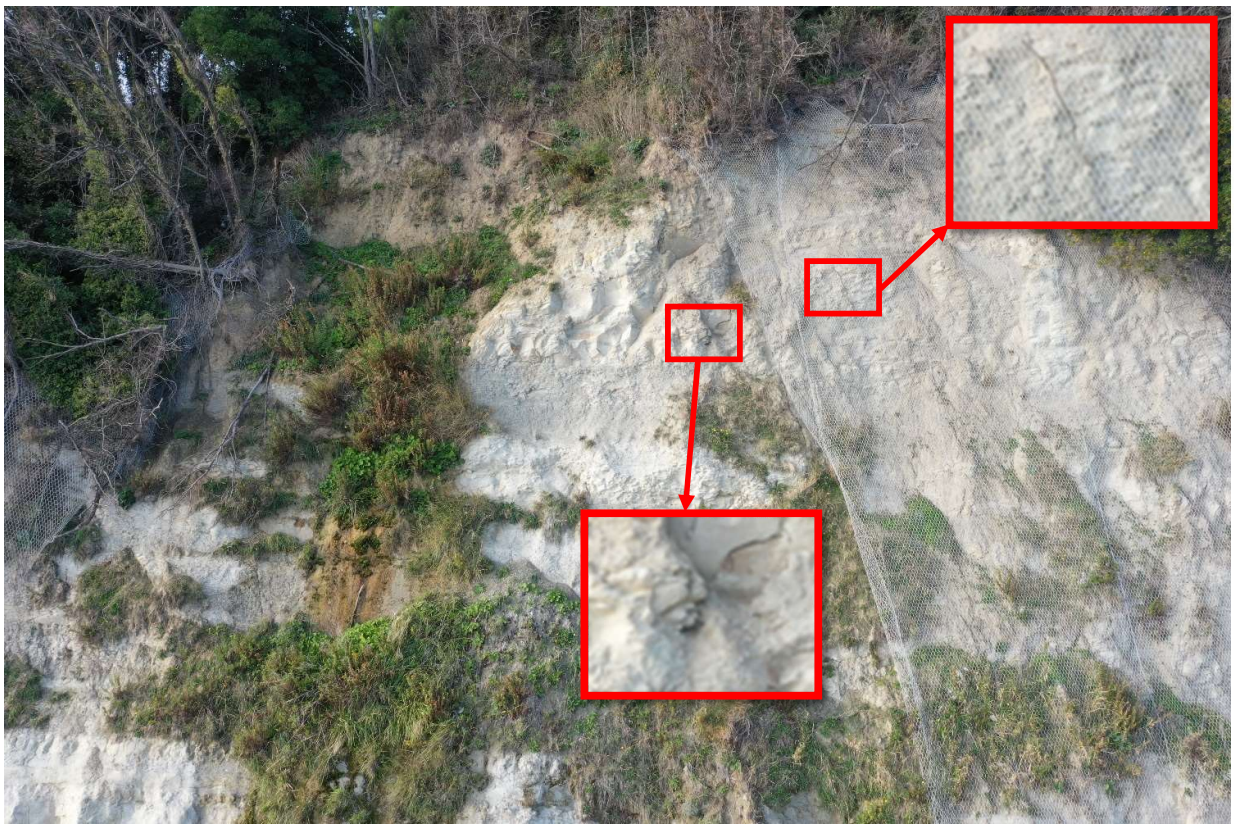

Figure 21 - Ground Control Points (GCPs) impossible to reach.

Total station data were referenced through a GPS survey, undertaken using a Trimble R8 GPS.

The GPS's measurement accuracy was about 2 cm using Real-Time Kinematic mode.

RTK is a positioning technique that solves accuracy, motion, and timing challenges, enabling satellite positioning systems to deliver highly precise location information.

5.4 Softwares and methods used for the data processing

5.4.1 3D sea cliff model generation – Metashape software

UAV photographs and GCPs were processed using the Agisoft Metashape software in order to generate 3D spatial data (Agisoft Metashape User Manual, Professional edition, Version 1.5, 2018).

The Metashape workflow consists of several key steps that are typically followed to process images and generate 3D models or orthophotos:

1. Uploading photos into Agisoft Metashape;
2. Inspect uploaded photos and remove unnecessary ones;
3. Aligning photos (Figure 22);
4. Introduction of markers with known coordinates (longitude, latitude, altitude);
5. Place Markers on the known points (ground control points) on the photos;
6. Review markers, review errors, discard the markers with greater error;
7. Build Point cloud;
8. Build Dense cloud;
9. Mesh construction (polygonal 3D model);
10. Texture Creation, Area Definition;
11. Build TILED Model;
12. Creating a Digital Elevation Model (DEM);
13. Creating orthophotos;
14. Exporting Results.

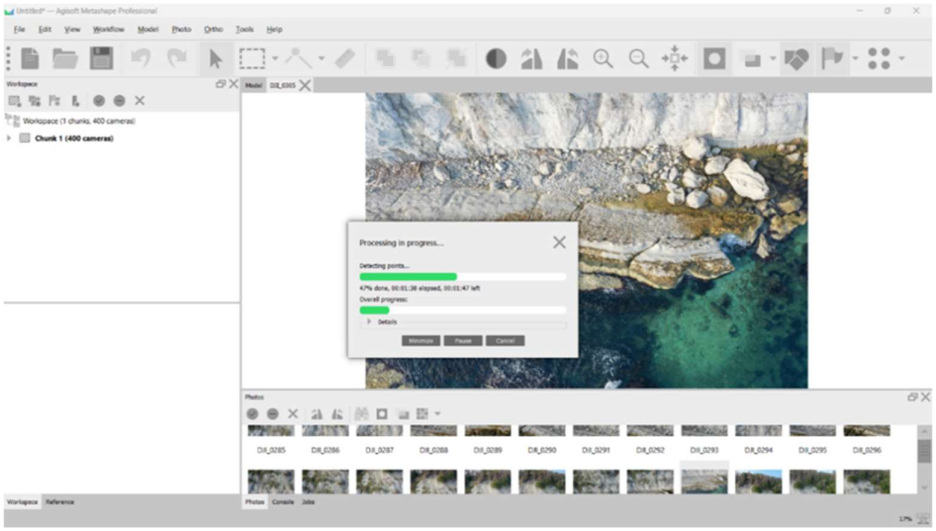

Figure 22 - Alignment of the photos.

The first step is to start Metashape and import the UAV photos into the project. It can be done by going to "File" > "Import Photos" and selecting the desired images. Then Metashape will attempt to estimate the position and orientation of imported images. The "Align Photos" option refines the orientation of the images. In the alignment phase of the cameras, Metashape identifies a series of common points on the photographs and associates them. This generates a point cloud scattered to a set of grip points (Figure 23). A point cloud is a collection of individual data points that represent the surface or structure of an object in 3D space. Each point in the cloud is defined by its coordinates (x, y, z) and may also contain additional attributes such as color or intensity.

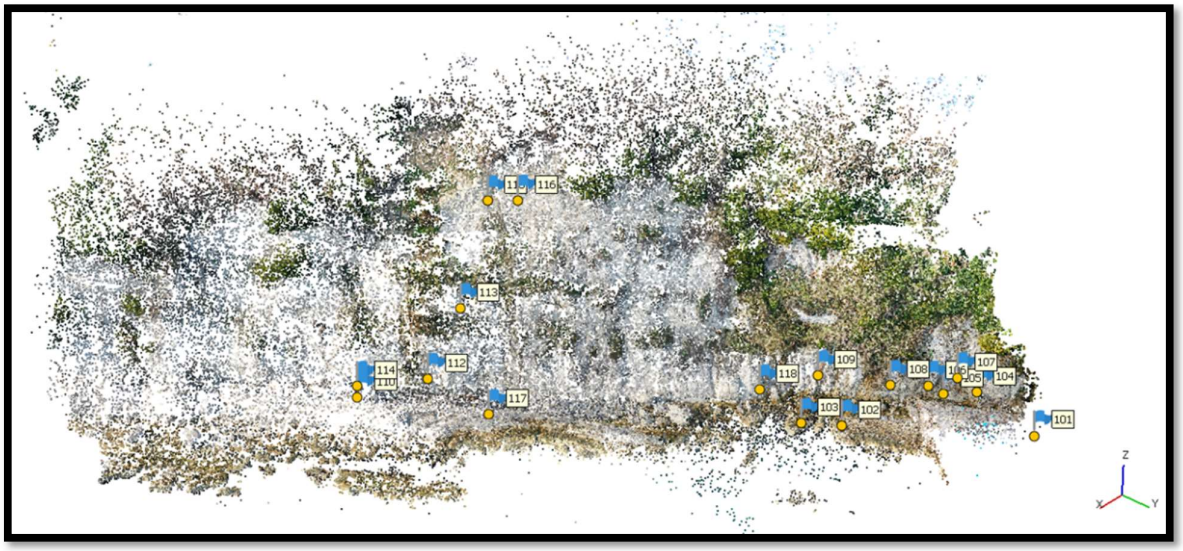

Figure 23 - Point cloud generation.

The scattered point cloud represents the starting result and allows you to get the rest of the products returned by the program.

The parameters that Metashape allows you to adjust during alignment are:

- Accuracy: Higher accuracy helps to achieve greater precision in estimating the position of grip points.
- Pair Selection: The process of aligning very large images can be time-consuming. A significant part of this time is spent matching the points between the photographs. The Pair Selection option is aimed at accelerating this phase by making the selection starting from the subset of pairs of points to be paired.
- Key point limit: The number entered imposes a limit of characteristic points recognized during alignment for each image. Setting the parameter to 0 uses as many points as possible while increasing the processing time and risking finding unstable points.
- Tie point limit: The number indicates the limit of pairs of points used for each image. If set to zero, the filter is bypassed.
- Adaptive camera model fitting: This option enables automatic processing of correction parameters related to the camera (internal orientation). The parameters that Metashape defines are focal length, position of the main points, three radial distortion coefficients (K1, K2, K3) and two tangential distortion coefficients (P1, P2).

Next, Metashape generates a dense point cloud (Figure 24). A dense cloud, also known as a "dense point cloud" or "point cloud reconstruction," is an improved version of a point cloud where additional points are added to increase the level of detail and accuracy. It is usually generated by performing post-processing algorithms on a raw point cloud, such as refining the alignment or filling in gaps. Each dense point cloud can be edited and classified within Metashape or exported to other external software for further analysis. The parameters that Metashape allows you to adjust to carry out for the construction of a dense point cloud are:

- Quality: Specifies the desired reconstruction quality. High quality settings can be used to achieve more detailed solutions with more accurate geometry but take longer to process.
- Depth filtering modes: When generating the dense point cloud, Metashape calculates depth maps for each image. Due to disturbing factors such as poor image quality, presence of noise or poor detail, some outliers can be generated. To resolve incorrect values, Metashape has several algorithms that act by filtering the information, with respect to the complexity of the geometry.

Figure 24 - Dense cloud generation

Now Metashape can reconstruct polygonal mesh model based on the point cloud information. A mesh is a surface representation of a 3D object created by connecting a series of vertices, edges, and faces. It is composed of polygons, such as triangles or quads, which define the shape of the object's surface. Once the mesh is generated Metashape will apply the original images to the surface of the mesh, creating a textured 3D model (Figure 25). Texture refers to the application of an image or pattern onto the surface of a 3D object. Texturing adds visual details such as color, patterns, or material properties to enhance the realism of a 3D model.

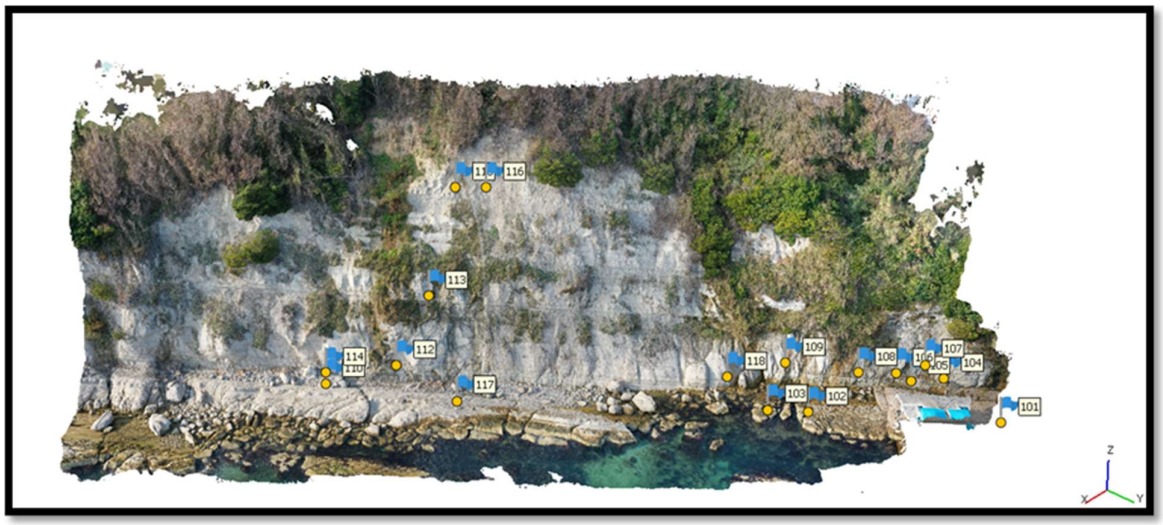

Figure 25 - Textured 3D model.

Finally, we are able to construct the 3D model and extract the orthophotos of the sea cliff. The 3D model (Figure 26) is a digital representation of a physical object in three dimensions. It includes the geometry, topology, and other attributes that describe the object's shape, structure, and appearance.

Figure 26 - 3D model of the cliff.

From the 3D sea cliff model and scanline investigation (chapter 5.1) we identified two sampling windows on which carry out our analyses (Figure 27). The sampling window is a portion of the rock mass that is considered for fracture analysis. Of course, the sampling window should be representative of the overall rock mass investigated: it should cover areas with varying lithologies, structural features, and stress conditions to provide a representative picture of the entire fracture system.

Figure 27 - Sampling windows: horizontal (red) and vertical (blue) portion of the cliff.

5.4.2 Fracture analysis - QGIS-Network GT

The technologies that have revolutionized the acquisition and management of geographic information are essentially three:

1) GNSS (global navigation satellite system): a communications system between ground stations and a network of satellites that allows the localization of a point on the earth's surface with an increasing level of precision depending on the instrumentation in use. The applications are innumerable, and the technology is now in common use. The most sophisticated GPS stations now allow a topographical accuracy higher than that of optical-electronic instruments, combined with better ease of use.

2) Remote Sensing: a set of techniques for acquiring images or other types of data through surveys made at a distance from airplanes and satellites, with the development of data processing and analysis. Those who study nature in its various forms today have a mass of information (in archive and in real time) and a quantity of data that can also be interpreted dynamically.

3) GIS (Geographic Information Systems): an information technology that allows you to manage the data detected by the other two and many other information in a systematic way, allowing visualizations, processing and analysis that add further knowledge and that facilitate decisions in terms of design and management.

We focused our work on this last technology, the GIS, because it is the one that gives more possibilities in terms of applications, being very useful, in some cases indispensable, to many professional categories, that is to all those who work for the territory, to get to know it, preserve it, administer it, plan it, manage it, design it.

There are excellent free, open source and free software in the GIS field, such as QGIS, the software that we have used in this work. QGIS is an open-source GIS desktop application that allows to visualize, organize, analyse, and represent spatial data.

Talking about the different vector formats, there is a fundamental one: the shapefile.

The shapefile is a vector data storage format capable of recording the location, shape, and attributes of spatial entities. A shapefile is made up of multiple related files and contains only one class of objects, i.e., points, lines, or polygons. All the files that make-up the shapefile must have the same name and what differentiates them is the extension.

There must be at least three files:

1. filename.shp: is the file that contains the geometric information.

2. filename.dbf: is the file that contains the table information (attribute data).

3. filename.shx: is the index file, which allows you to link geometry and table information.

The set may also contain other files:

1. filename.prj: registers the Geographic Reference System.

2. filename.sbn (or also fbn, fbx): they record spatial indexes.

3. filename.ain (or aih): record attribute indexes.

4. filename.xml - Logs metadata.

In this work we used the plugin of QGIS, NetworkGT (Network Geometry and Typology) toolbox, that is a set of tools designed for the geometric and topological analysis of fracture networks in QGIS.

Björn Nyberg et al. (2018), with the paper "NetworkGT: A GIS tool for geometric and topological analysis of two-dimensional fracture networks" gave us a lot of information on the uses of this tool. Figure 28 shows the main step of the analysis.

It provides a range of tools that allows the user to utilize several traditional sampling methods to automatically conduct a robust characterization of the networks geometric and topological properties as well as assessing its spatial variability.

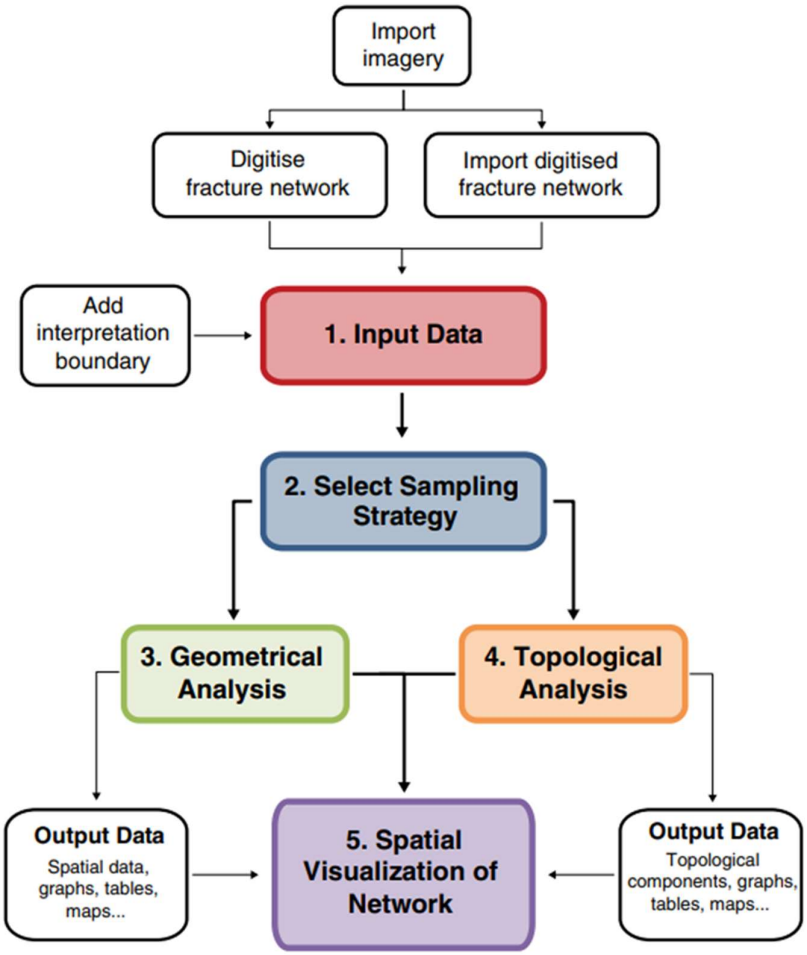

Figure 28 - Schematic workflow of the NetworkGT tool (Björn Nyberg et al., 2018).

NetworkGT helped us to identify the discontinuities: the fracture intensity parameter (P21, expressed as the length of fracture per unit area), and fracture network connectivity (small scale centimeter/millimeter fractures were not considered) were used to this purpose.

In a geomechanical survey of a rock mass is really difficult to find isolated fractures: more frequently they appear as a network of fractures whose arrangement, abundance, and interaction control the mechanical and transport properties of rock masses. Of particular importance are the distributions and spatial variations of different geometric (locations, orientation, length, etc.) and topological attributes (intersections, connectivity, etc.) of fractures in a network.

The fracture intensity parameter P21 is a quantitative measure used to evaluate the fracture density or intensity within a rock or geological formation. It is commonly used in the field of structural geology and geomechanics to characterize the presence and abundance of fractures within a given rock volume.

Regarding this parameter, the classical method allows to calculate it by dividing the total number of fractures by the surface area: it represents the average fracture density within the studied rock volume. In our case we calculated it using NetworkGT, defining multiple P21 values of several test circles and calculate an average value and its standard deviation.

In addition to the P21 value, the connectivity value was considered.

Fracture network connectivity refers to the degree to which fractures within a rock or geological formation are interconnected or linked together. It is a measure of how fluid flow, stress transfer, or other physical processes can propagate through the fracture system. The connectivity of a fracture network is influenced by various factors, including the density, orientation, size, and geometry of the fractures. Highly connected fracture networks allow fluids (such as water, oil, or gas) to flow more easily through the rock, while poorly connected networks restrict fluid movement. It was calculated by averaging several test circles for each sampling window.

A total of 18 test circles for each sampling window was used for the calculation of the P21 and connectivity values.

The result of the connectivity analysis provided lines, nodes, and branches between nodes for which a connectivity value could be calculated for each test circle:

- The individual fractures (lines) within the network. This includes details such as the orientation, length, and other properties of each fracture.
- The nodes represent the points where fractures intersect or terminate. In a fracture network, nodes can be categorized as intersection nodes (where two or more fractures intersect) or end nodes (where a fracture terminates).
- The branches refer to connected sets of fractures within the network. A branch consists of a series of fractures that are interconnected, either through intersecting fractures or through a continuous fracture path. Each branch represents a connected pathway within the fracture network.

5.4.3 Discrete Fracture Network (DFN) – Move Software

Understanding the behavior of fractures within the rock mass is critical for many engineering applications such as construction of buildings, tunnels, highways and, in our casa for groundwater investigation and management.

The construction of a Discrete Fracture Network (DFN) take place within the Move software, using the fracturing modeling module.

Move is a widely used software package for structural geology modelling developed by Midland Valley Exploration. It provides tools for creating and visualizing 3D geological models, including fault analysis, fracture modelling, and restoration techniques also integrating GIS data.

A DFN is a conceptual representation of the fractures present in a rock mass or subsurface formation. It is a model used in geology, hydrogeology, and engineering to understand and predict the behaviour of fractured systems.

It considers the geometry, orientation, and connectivity of fractures, along with their mechanical properties, such as aperture and permeability. By characterizing and analysing the DFN, it is possible to obtain information about fluid flow, stress distribution, and mechanical behaviour within fractured rock masses.

More in detail, the objective is to extract the value of hydraulic conductivity within the fracture system and compare it with the values obtained from the tracer test performed by Pepi (2021), mentioned before. In our case the hydraulic conductivity value is related to the ability of fractured rock to be crossed by a fluid: characteristics like fracture aperture and frequency, fracture length, fracture orientation and angle, fracture interconnectivity, filling materials, and fracture plane features are critical parameters for the estimation of the hydraulic conductivity.

Field observations, borehole data, geophysical surveys, and remote sensing data are commonly used to identify and characterize fractures. These data are then integrated to create a realistic representation of the fracture network. Once the DFN is constructed, it can be used for a wide range of applications: in hydrogeology, DFN help in simulating groundwater flow and contaminant transport through fractures; in geotechnical engineering is used to understand the stability of rock slopes and the behaviour of underground excavations.

So, for understanding and simulating the behaviour of fractured rocks the discrete fracture network modelling is a valid tool.

Considering all the information obtained, 3D DFN model was set up using the fracture modelling module of MOVE software (academic license provided by Petroleum Experts Ltd. to the University of Camerino).

This fracture modelling module is designed for tight rocks where porosity and permeability are guaranteed only by the fracture pattern. The software assigns zero values of porosity to the portions of the rock volume that are not crosscut by any fracture.

This methodology has been recently applied by other authors (Antonellini et al., 2014; Panza et al., 2015, 2016; Zambrano et al., 2016).

The following input data, for each fracture set, are considered to set up the model:

- the orientation (expressed as dip azimuth, dip angle, and Fisher K value).
- aspect ratio (height/length).
- length distribution.
- hydraulic aperture.
- volumetric fracture intensity (P32).

The hydraulic aperture is derived from the mechanical aperture, which is measured in the field using the JRC profile – aperture comparator (Figure 29) (Barton & Choubey, 1977).

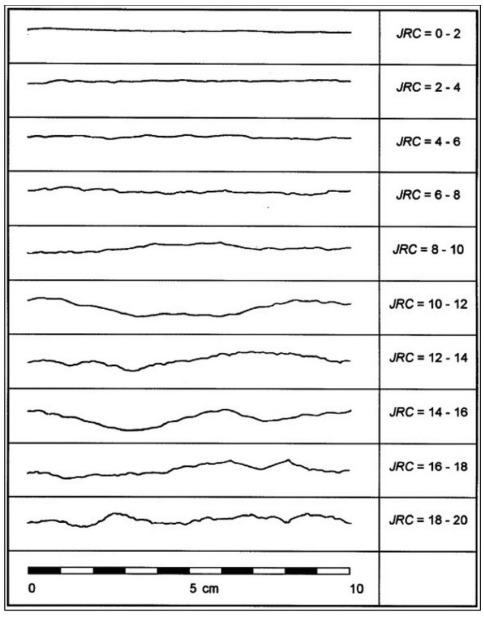

Figure 29 - JRC profile (Barton & Choubey, 1977).

We estimated the JRC by visually comparing the fractures with standard set of roughness profiles. The hydraulic aperture, “e”, is the idealized fracture aperture for smooth parallel plates model (Snow, 1965) and was derived from Zambrano et al. (2019).

An aspect (length:height) ratio of 2 was assumed (Cowie & Scholz, 1992); (Olson, 2003); (Scholz, 2010).

The P32 value represents the volumetric fracture intensity (area of fractures per unit volume) and was obtained following an iterative approach. The discrete fracture network models were created using random values of P32. In these models, for each fracture set, using 2D pseudo-scanlines (cross sections of the DFN) the average value of P21 was calculated.

The discrete fracture network was developed using a 12 × 12 m box to have a pretty accurate but not complex model to work on.

6. Results

6.1 Fracture sets orientation

Based on the conventional geomechanical analysis (scanline method) and UAV survey, average fracture set orientation and characteristics were identified.

Field observations of the rock mass were essential for identifying and characterizing fractures. This involves visually inspecting the rock surface, outcrops, or underground exposures to identify fractures and their attributes.

Certainly, the only observation is not enough to have a complete picture of the area. For this reason, the use of the scanline was fundamental: fractures intersecting the scanlines were recorded and analysed to identify distinct fracture sets based on orientation data.

Then the drone survey provided detailed topographic and imagery data helping in identifying fractures and their orientations, as well as mapping fracture sets.

From the geomechanical scanline method survey and UAV model analysis we extracted the stereographic projection using the RocScience software DIPS. Three main joint sets were identified, respectively named J1, J2, and J3 and the bedding plane S0 (Figure 30).

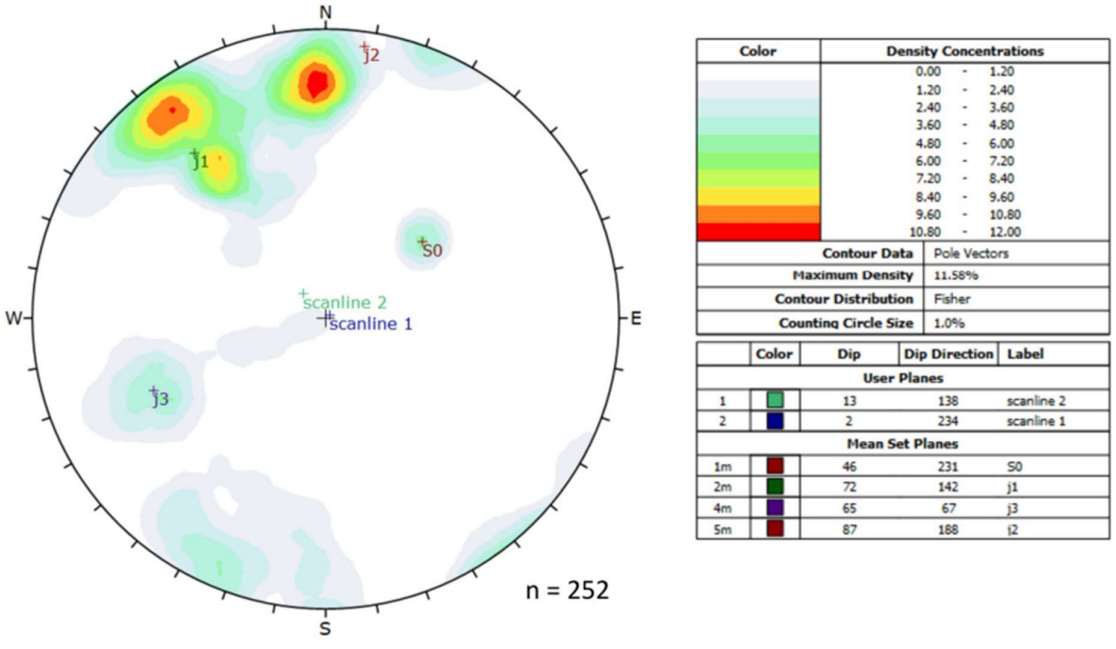

Figure 30 - Stereonet with pole vector plot (lower emisphere, equal angle) with indication of mean set dip angle and dip direction of the planes.

6.2 3D sea cliff model and orthophotos

Figure 31 shows the result of the Metashape workflow, the 3D model of the sea cliff.

Figure 31 - 3D model of the cliff.

Based on the information obtained from scanline and UAV survey, we identified two sampling windows. Then, from the 3D model we extracted the two orthophotos of the respective sampling windows.

An orthophoto is a satellite image corrected in terms of geometry to remove distortions caused by terrain relief, camera tilt, and other factors making it suitable for accurate measurements, mapping, and analysis.

For the creation of the orthophotos the “build orthomosaic” option was selected from the workflow menu. Then Metashape combined the photos together, aligning them based on the dense point cloud and removing distortions caused by perspective and terrain variations.

In this way georeferenced orthophotos (Figure 32 and Figure 33) are obtained, visualized within the software and exported in various file formats like TIFF, JPEG, or GeoTIFF, which can be used in GIS or other software for other analysis or visualization.

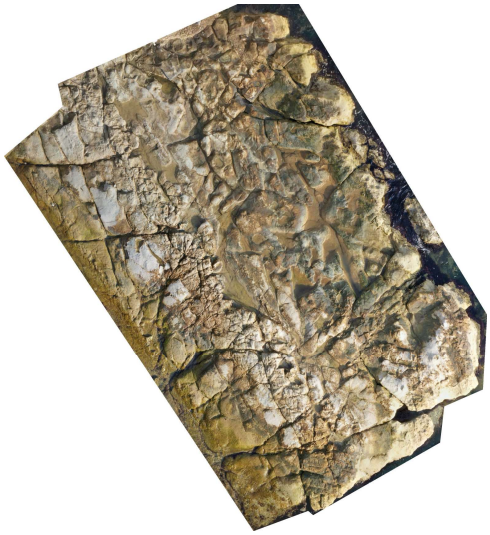

Figure 32 - Orthophoto of the sampling window 1.

Figure 33 - Orthophoto of the sampling window 2.

Two further tests were carried out through independent check measurements, to validate the 3D model.

In the first test, the distance between two GCPs was measured by the total station and the 3D UAV-extracted model. The second test was based on the comparison between the fracture orientation measured in the field with a geological compass and in the 3D model. Results of independent check measurements are reported in Table 1, highlighting the good correspondence between the UAV-extracted data and independent measurements.

Total Station Measurement	**3D Model**
64.472	64.458
compass measurement of dip and dip direction (degrees)	**3D model-extracted dip and dip direction (degrees)**
65/67	60/68

Table 1 - Independent check measurements.

6.3 Fracture analysis results

The results of the geomechanical survey are reported in Table 2: average orientation of the joint sets, Fisher values, fracture trace length, mechanical and hydraulic aperture. The bedding planes (S0) were tightly closed; thus, they were assumed as negligible for the scope of the fluid flow, so, not included in the following DFN modelling.

		J1	J2	J3	S0
Dip angle/Dip direction (°)		71/141	88/188	65/67	46/231
Fischer value		25.9	14	81	867
Fracture trace length (m)	Min	0.2	0.2	0.18	n.d.
	Mean	1.82	1.60	2.22	n.d.
	Max	12.46	11.32	13.87	n.d.
	Std. Dev	2.06	2.14	2.86	n.d.
Hydraulic aperture (mm)	Min	0.18	0.12	0.18	n.d.
	Mean	0.24	0.19	0.25	n.d.
	Max	0.95	0.5	0.5	n.d.
Mechanical aperture (mm)	Min	0.90	0.70	0.90	n.d.
	Mean	0.95	0.85	1.00	n.d.
	Max	2.60	1.80	1.80	n.d.

Table 2 - Discontinuities set characteristics from the geomechanical survey.

The following figure shows the fracture analysis in sampling window 1 (Figure 34, a) and the resultant connectivity values in the ternary graphs (Figure 34, b). The same for the sampling window 2 (Figure 35: a, b). It is important to remember that the analysis has been carried out in multiple 1 square meter areas for each sampling window and therefore different values of connectivity have been calculated for each window.

The sampling windows present high connectivity values, with the sampling window 1 having the highest ones. The nodes of the fracture system are classified as:

- isolated nodes (I) nodes
- connecting nodes (Y or X)

The branches are classified as:

- I-I=isolated-isolated branches
- C-C=connected-connected branches
- C-I=connected=isolated branches

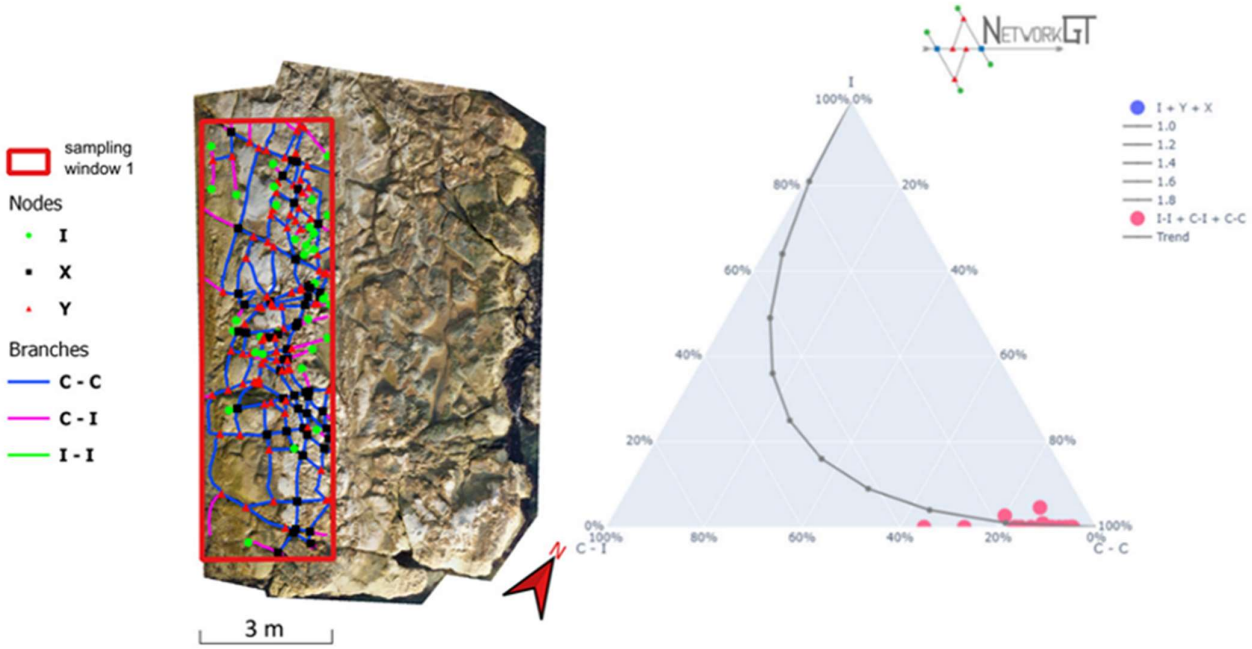

Figure 34 - Sampling window 1: Fracture analysis (a); ternary graph with connectivity values (b).

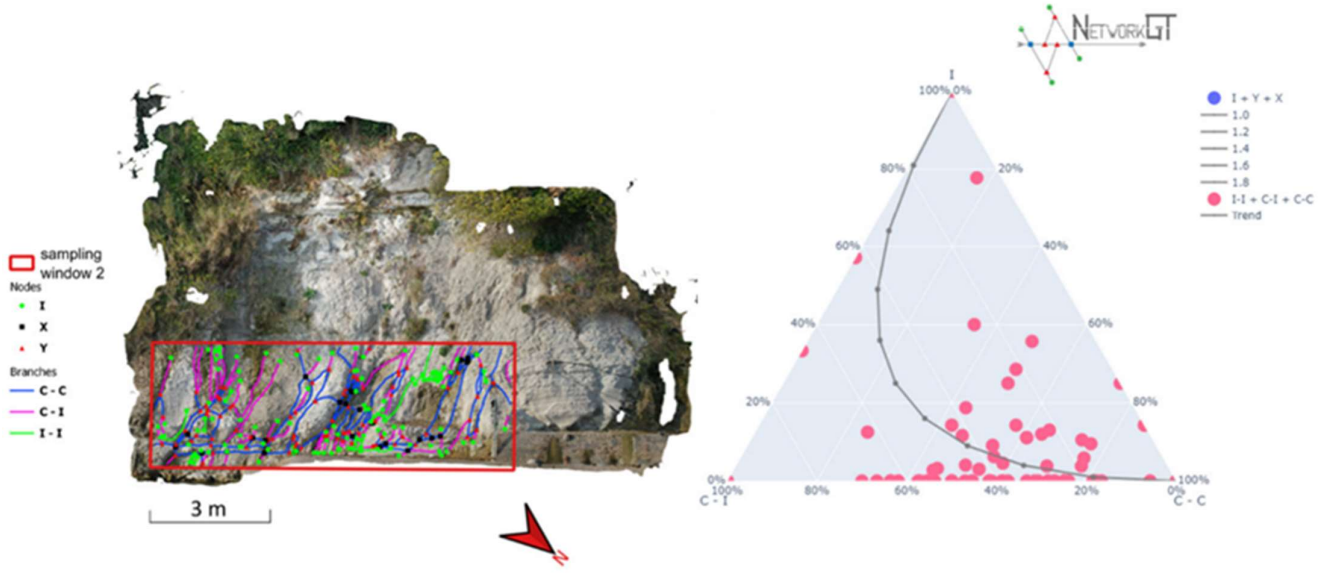

Figure 35 - Sampling window 2: Fracture analysis (a); ternary graph with connectivity values (b).

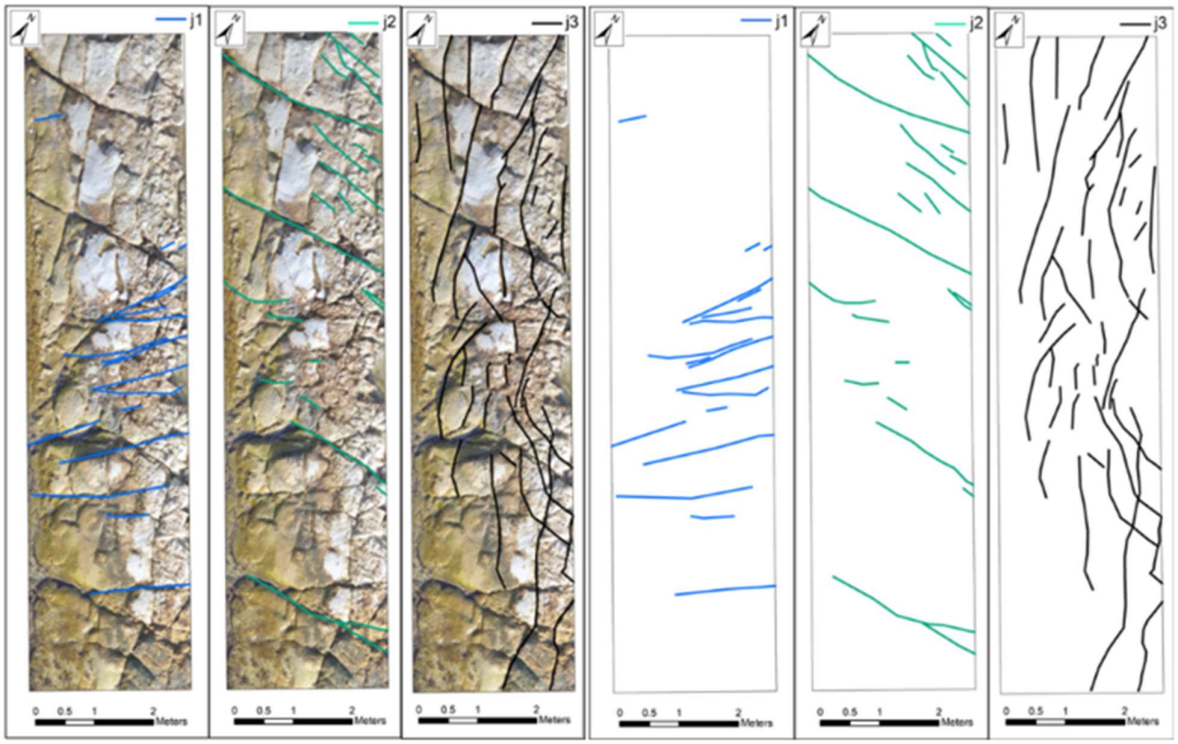

Figure 36 - Fracture analysis performed in NetworkGT for fracture set J1, J2, J3 of sampling window 1, with and without orthophoto.

The figure 36 (above) shows the fractures used for the calculation of the P21 values in NetworkGT (with and without the orthophoto base map, respectively).

The results for the P21 from sampling window 1 are:

- J1: 0.96 m/m^2
- J2: 0.74 m/m^2
- J3: 1.89 m/m^2.

6.4 DFN model creation and validation

The construction of the discrete fracture network followed an iterative approach aimed at obtaining sections with fracturing intensities comparable to those parameterized inside the wall windows.

The DFN was built by separately modelling 3 sets of discontinuities detected with scanlines and UAV analysis. Although from the conventional geomechanical analysis, three joint sets and one bedding plane have been evidenced, the DFN model was developed only with joint set J1, J2 and J3. The reason lies in the fact that the bedding is close and dipping towards upstream (Table 2). Only once the results obtained from the modelling of each of these sets of discontinuities were validated, the final DFN was created.

The discrete fracture network was developed using an iterative approach: the input P32 was changed until the P21 matched the ones of the sampling windows.

Table 3 report:

- P21 obtained from the sampling windows;
- P21 obtained from DFN;
- P32 obtained from the iterative approach;

	J1	J2	J3	S0
Mean P21 (sampling window 1, m/m^2)	0.96	0.74	1.89	n.d.
Mean P21 from the DFN (m/m^2)	0.91	0.87	1.90	n.d.
Fracture intensity P32 (m^2/m^3)	0.8	0.5	1.8	n.d.

Table 3 - Fracture intensity analysis from the sampling windows and DFN model. n.d. = not detected.

After the iterative approach mentioned above, it is possible to note the correspondence between the values of P21 obtained from the sampling windows with the ones gathered from the DFN.

An example of this approach is reported in the next page: the green “scanline” selected and extracted as a section of the DFN (Figure 37) was used to evaluate the fractures and calculate the P21 (Figure 38).

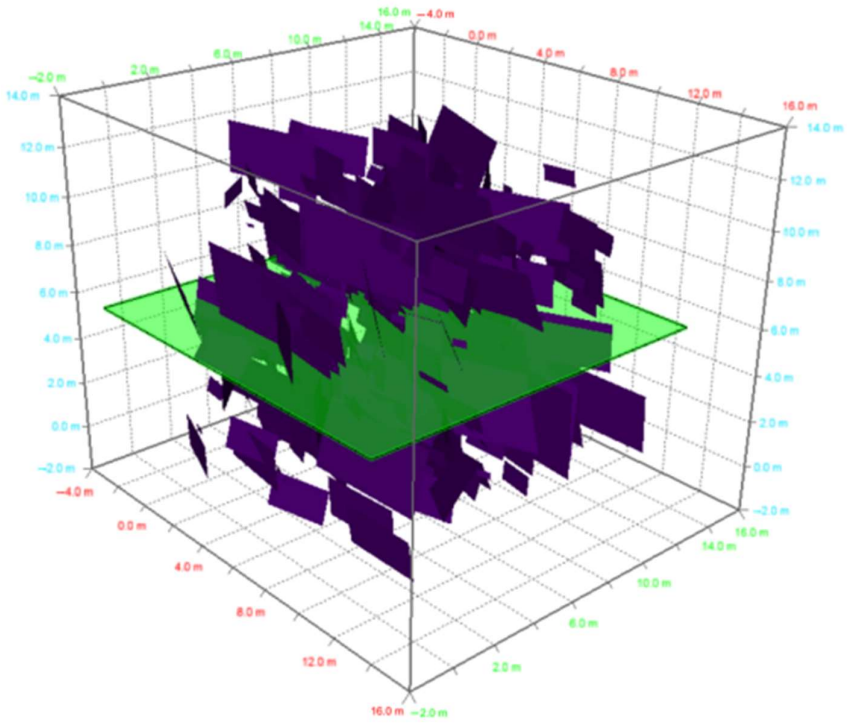

Figure 37 - Pseudo-scanline creation (green) in the initial Discrete Fracture Network model.

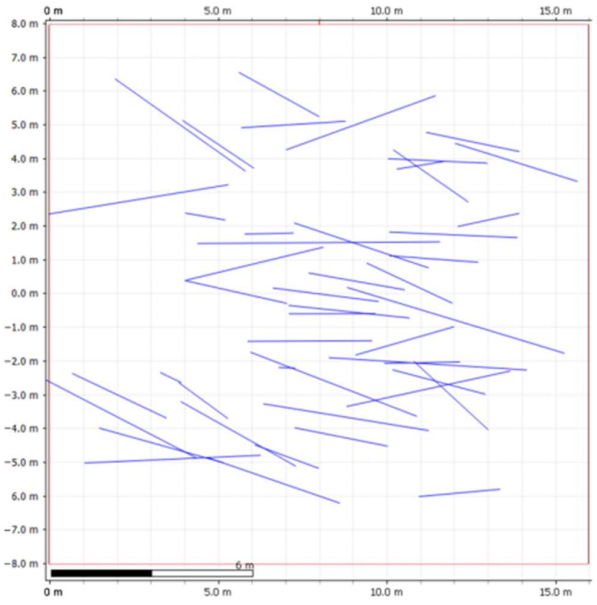

Figure 38 - Pseudo-scanlines extracted from the DFN and used to calculate P21.

After obtaining sections comparable to the sampling windows, the 3 sets of discontinuities were integrated within a single DFN model. Figure 39 highlights the DFN model developed after the iterative approach and figure 40 shows the pseudo-scanline extracted from the DFN and imported in NetworkGT for the validation procedure.

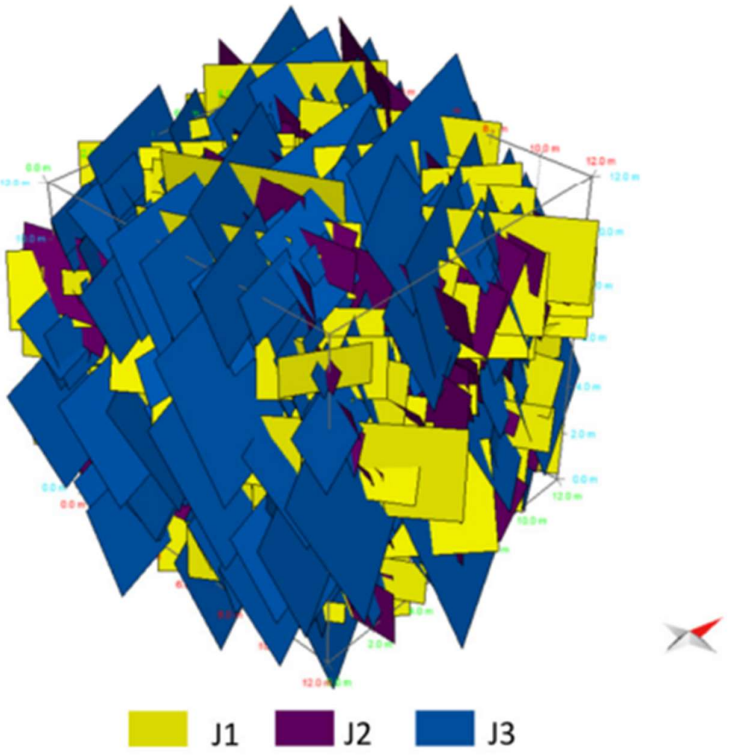

Figure 39 - DFN model developed after the iterative approach.

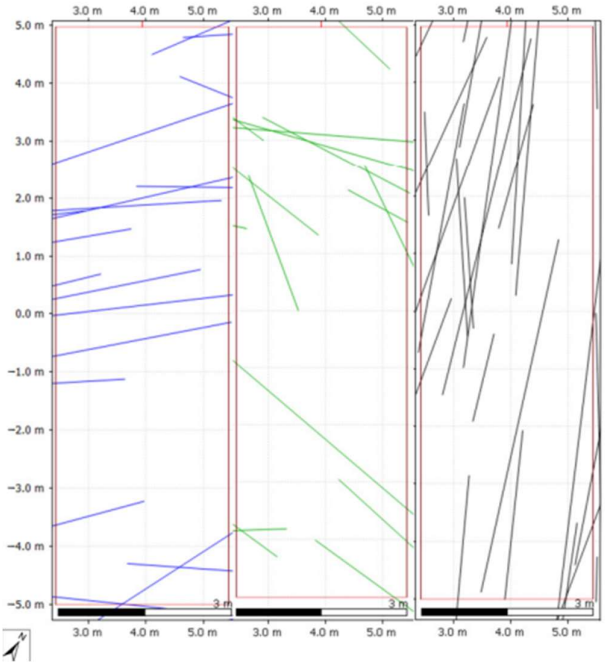

Figure 40 - Pseudo-scanline extracted from the DFN and imported in NetworkGT for the validation.

It is possible to note the correspondence between the fractures extracted from the DFN (Figure 40, above) and the fractures obtained after the NetworkGT analysis (Figure 36).

From the DFN model it was possible to extract the fracture conductivity (k), equal to 2.91×10^{-3} cm/s.

7. Discussion

The methodology presented in this work followed a multi-disciplinary approach integrating different types of survey and analysis techniques: scanline method, UAV survey, geometric and topological analysis of fractures, DFN modelling.

These techniques are often used in the field to investigate, analyse, and solve engineering geology problems. These problems refer to a progressive degradation of the soil, caused both by nature and by human action. So, the conformation of a given area or territory and the occurrence of natural events certainly play an important role, but also human, with his intervention, contributes to increasing this instability.

Specifically, the natural factors that most of all influence the instability of a slope are certainly the geology and morphology of the soil, the rock mass fracture system and the groundwater circulation, in addition to sea erosion at the cliff base.

Human increases these phenomena with the construction of buildings, excavations, deforestation, interventions on waterways: all actions that strain the stability of an area.

We often intervene only after these phenomena have occurred, trying to counteract with the construction of artifacts. What is lacking, in most cases, is the prevention of risks, the prevention of these phenomena from occurring or, at least, the reduction of possible damages. This prevention, certainly more effective, however, requires careful arrangement of risk areas, to be implemented after an adequate hydrogeological and geomechanical study. In addition, the triggering factors of rock fall or landslide in general are fundamental to understand the mechanical behavior and predict the activation time in future.

In the framework of geomechanical survey in inaccessible or partially accessible areas and due to the steepness of the cliff, the use of geomatic techniques is critical; in fact, the scanline survey can be used only at the cliff base and in areas in which the required minimum length of 10-12 m can be satisfied.

In this regard, Mammoliti et al. (2022) evidenced the change in the litostratigraphic sequence within the Schlier Fm. In the Cardeto area (Ancona, Marche Region), in which the spacing measured from the laser scanner techniques evidenced a slightly variation in its value from the bottom to the top of the cliff. Moreover, the amount of data that can be collected using geomatic techniques such as laser scanner, UAV survey etc. is several orders of magnitude greater than the conventional geomechanical

survey. These problems have been overcome integrating the conventional surveys with unmanned aerial vehicle (UAV) system.

An example of this type of work is given by Francioni et al. (2020) and Tuckey (2022) who explained the importance of data from UAV in the investigation, analysis, and evaluation of the fracture network.

Francioni et al. (2020), proved the improvement on the investigation of inaccessible high steep slopes with the use of the drone for the definition of fracture properties like intensity, block volumes, and rockfall trajectories. Tuckey (2022) studied the utility on the use of models generated from the images collected with the drone for the estimation of geo-mechanical parameters regarding the fracture system: in this way it was possible to create a complete and detailed DFN. However, in the literature any study is given to couple DFN with tracer tests to investigate the hydraulic conductivity of the discontinuities. For this reason, this study was a great contribution to the knowledge of groundwater circulation in a fractured rock cliff in a portion of Passetto (Ancona, Italy), that is known to be subjected to rock fall kinematics (Mammoliti et al. 2023), and in which the groundwater circulation plays a fundamental role in the rock collapse. The mentioned area, characterized by outcropping of the Schlier geological formation, presents a high fracturing, that in addition to erosion from the sea contribute to the general instability.

This multi-level survey has led to a substantial increase in the available data, making the subsequent analysis complete and detailed, as well as the final results. Thanks to the geomechanical suvey, three different joint set and the bedding were identified. The results of the geomechanical survey provided: a) average orientation of the joint sets; b) Fisher values; c) fracture roughness; d) fracture trace length; e) mechanical and hydraulic aperture. Due to the different orientations (dip angle /dip direction) of the joint sets in the rock mass, two sampling windows are necessary to better represent the fracture system. In details, the sampling window 1 successfully highlights the fracture set j3, that is striking parallel to the sea cliff wall. In this way is possible to measure all the discontinuity characteristics of fracture set j3, including spacing that is impossible to be collected in sampling window 2 (vertical portion of the cliff). The bedding is the only one figuring out totally close (aperture = 0).

Thanks to the images acquired through the UAV technique and processed into Agisoft Metashape, it was possible to reconstruct a digital representation of the entire cliff in three dimensions: the 3D model. From the 3D model, two orthophotos derived from the two sampling windows were obtained, and thus, thanks to the NetworkGT tool of QGIS, it was possible to perform a fracture analysis by integrating UAV-based and scanline results. Fractures sets and their characteristics were identified and assessed through the combination of these methods.

Then, using all the information gained from the previous fracture analysis as an input, we created the DFN, a 3D computational fractures representation present in a rock volume; it represents in detail the characteristics of fractures, including their orientation, length, aperture and spatial distribution. Due to the fact that the bedding is close and dipping towards upstream, the DFN was implemented only considering fracture set J1, J2 and J3. In the process of creating and validating the DFN we compared the fracture system and the P21 values obtained from the results from NetworkGT and those derived from the DFN, obtaining an excellent matching (Figure 41 and Table 4).

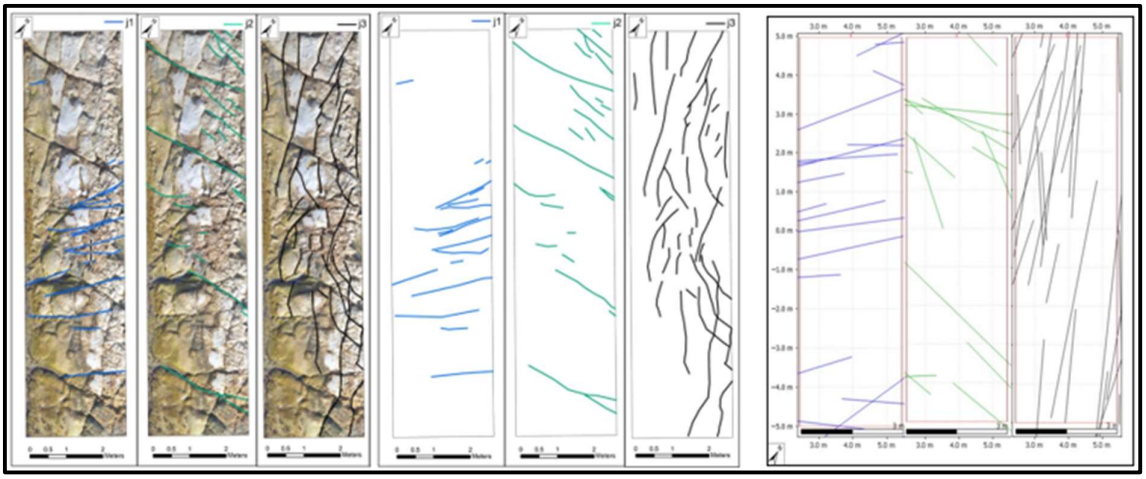

Figure 41 - Comparison between the fractures extracted from Network GT and DFN.

		J1	J2	J3
P21 from Network GT	[m/m^2]	0.96	0.74	1.89
P21 from DFN	[m/m^2]	0.91	0.87	1.90

Table 4 - P21 values comparison between NetworkGT and DFN.

Moreover, the results obtained from the DFN were compared with data obtained from tracer tests carried out in the same area by Pepi (2021), with the aim of validate the hydraulic conductivity derived from the DFN and improve the rock slope instability investigations. These two methods, DFN and tracer test, which are usually involved separately in different disciplines, are here combined in order to propose an innovative methodology for hydro-geomechanical studies. Comparing the results of the fractures hydraulic conductivity (K) derived from the DFN modelling and tracer test, a very good correspondence is evidenced in Table 5.

		Average K (cm/s)
DFN	fractures	2.91 x 10^{-3}
Tracer Test (Pepi, 2021; Mammoliti et al., 2023)	fractures	2.89 x 10^{-3}
	topsoil	1.8 x 10^{-2}

Table 5 - Results of conductivity (K) derived from the DFN model and tracer tests for the topsoil and fractures.

8. Conclusions

The aim of this thesis was to provide a multi-level approach aimed at the analysis of a portion of the cliff in the Passetto area in Ancona, characterized by a strong structural instability due to high fracturing grade and the high hydraulic conductivity calculated in this work. In addition, rock type, the high slope of the cliffs, and the sea erosion at the cliff base are contributing factors to its instability.

Following, the main highlights of the thesis are listed:

- Due to the inaccessibility of some areas, the traditional investigation methods could be difficult and unsafe. In addition, classical geomechanical surveys does not always allow to obtain the representative quantity of data in some contexts and collect data in a reasonable short time period. These issues have been overcome with the combined use of conventional surveys and drone detection, greatly increasing the amount of data in otherwise inaccessible areas;
- From the images collected with the UAV methodology, a 3D model of the rock mass was created starting from a point cloud in order to have a better representation of the entire outcrop; two representative sampling windows were identified and extracted as orthophotos to be analysed;
- With NetworkGT it was possible to make a deeper investigation of the fracture system such as the fracture intensity parameter P21 and fracture network connectivity, that are critical parameters for the groundwater circulation. The sampling windows analysed both presented high connectivity values that strengthen the assumptions;
- With this information it was possible to create and validate a DFN. The use of DFN modelling was crucial in understanding the fracture system and the groundwater pattern.
- A very good correspondence was obtained between the fracture analysis in NetworkGT and the DFN, validating the results;
- From the DFN, the conductivity value was extracted. This value was validated by comparing it with the results obtained from the tracer test made by Pepi (2021) obtaining an excellent correspondence.

The combination of surveying with traditional methods and drones has been widely studied, also in literature. The combination of this methodology with tracer tests represents a new investigative approach, worthy of further deepening and tests.

This thesis has contributed to the collection and interpretation of data of the published scientific paper named “3D Discrete Fracture Network Modelling from UAV Imagery Coupled with Tracer Tests to Assess Fracture Conductivity in an Unstable Rock Slope: Implications for Rockfall Phenomena” authored by Mammoliti et al. (2023).

Bibliography

Adler, P.M.; Thovert, J.-F.; Mourzenko, V.V. Fractured Porous Media; Oxford University Press: Oxford, UK, 2013; ISBN 0-19-966651-2.

Althaus, E.; Friz-Töpfer, A.; Lempp, C.; Natau, O. Effects of Water on Strength and Failure Mode of Coarse-Grained Granites at 300 C. Rock Mech. Rock Eng. 1994, 27, 1–21.

Aringoli, D., Gentili, B., Materazzi, M., & Pambianchi, G. (2010). Landslides: Causes, Types and Effects Mass movements in adriatic central Italy: activation and evolutive control factors.

Aringoli, D., Gentili, B., Materazzi, M., Pambianchi, G., & Farabollini, P. (2014). Il ruolo della gravità nell'evoluzione geomorfologica di un'area di falesia: Il caso del Monte Conero (Mare Adriatico, Italia centrale). 14.

Barton, N.; Choubey, V. The Shear Strength of Rock Joints in Theory and Practice. Rock Mech. 1977, 10, 1–54.

Berkowitz, B. Characterizing Flow and Transport in Fractured Geological Media: A Review. Adv. Water Resour. 2002, 25, 861–884.

Camanni, G.; Vinci, F.; Tavani, S.; Ferrandino, V.; Mazzoli, S.; Corradetti, A.; Parente, M.; Iannace, A. Fracture Density Variations within a Reservoir-Scale Normal Fault Zone: A Case Study from Shallow-Water Carbonates of Southern Italy. J. Struct. Geol. 2021, 151, 104432.

Carminati, E., & Doglioni, C. (2012). Alps vs. Apennines: The paradigm of a tectonically asymmetric Earth. Earth-Science Reviews, 112(1–2), 67–96.

Casagli, N.; Garzonio, C.A.; Nanni, T. Geomechanical Characterization and Slope Instability of the Marly Sea Cliffs of Ancona, Italy. In Proceedings of the Geotechnical Engineering of Hard Soils-Soft Rocks, Athens, Greece, 20–23 September 1993; pp. 1093–1100.

Chen, G.; Illman, W.A.; Thompson, D.L.; Vesselinov, V.V.; Neuman, S.P. Geostatistical, Type-Curve, and Inverse Analyses of Pneumatic Injection Tests in Unsaturated Fractured Tuffs at the Apache Leap Research Site near Superior, Arizona. In Dynamics of Fluids in Fractured Rock; Blackwell Publishing Ltd.: Oxford, UK, 2000; pp. 73–98.

Coltorti, M.; Nanni, La pericolosità geologica in un'area in rapido sviluppo urbanistico: il tratto di costa tra Ancona Nord e il fiume Esino. 1987.

Corradetti, A.; Tavani, S.; Parente, M.; Iannace, A.; Vinci, F.; Pirmez, C.; Torrieri, S.; Giorgioni, M.; Pignalosa, A.; Mazzoli, S. Distribution and Arrest of Vertical Through-Going Joints in a Seismic-Scale Carbonate Platform Exposure (Sorrento Peninsula, Italy): Insights from Integrating Field Survey and Digital Outcrop Model. J. Struct. Geol. 2018, 108, 121–136.

Colosimo, P. (1973). Carta geolitologica ad orientamento geotecnico e della franosità della zona del monte Conero (Comuni di Ancona, Numana, Sirolo).

Cowie, P.A.; Scholz, C.H. Displacement-Length Scaling Relationship for Faults: Data Synthesis and Discussion. J. Struct. Geol. 1992, 14, 1149–1156.

Crescenti, U.; Dattilo, G.; Massa, G.; (1978). Note di geologia tecnica nel territorio di Ancona. Studi Geologici Camerti, 4: 67-73.

Daniela, R.; Ermanno, M.; Antonio, P.; Pasquale, R.; Marco, V. Assessment of Tuff Sea Cliff Stability Integrating Geological Surveys and Remote Sensing. Case History from Ventotene Island (Southern Italy). Remote Sens. 2020, 12, 2006.

Dershowitz, W.S.; Herda, H.H. Interpretation of Fracture Spacing and Intensity. In Proceedings of the 33rd US Symposium on Rock Mechanics (USRMS), Santa Fe, NM, USA, 8–10 June 1992.

Devoto, S.; Macovaz, V.; Mantovani, M.; Soldati, M.; Furlani, S. Advantages of Using UAV Digital Photogrammetry in the Study of Slow-Moving Coastal Landslides. Remote Sens. 2020, 12, 3566.

Dubbini, A., Guerrera, F., Sandroni, P. Nuovi dati sullo Schlier dell'Appennino umbro-marchigiano. Giorn. Geol, 53(2), 115–130.

Feng, Q.H.; Röshoff, K. In-Situ Mapping and Documentation of Rock Faces Using a Full-Coverage 3d Laser Scanning Technique. Int. J. Rock Mech. Min. Sci. 2004, 41, 139–144.

Fisher, R.A. Dispersion on a Sphere. Proc. R. Soc. Lond. Ser. Math. Phys. Sci. 1953, 217, 295–305.

Francioni, M.; Antonaci, F.; Sciarra, N.; Robiati, C.; Coggan, J.; Stead, D.; Calamita, F. Application of Unmanned Aerial Vehicle Data and Discrete Fracture Network Models for Improved Rockfall Simulations. Remote Sens. 2020, 12, 2053.

Fronzi, D.; Di Curzio, D.; Rusi, S.; Valigi, D.; Tazioli, A. Comparison between Periodic Tracer Tests and Time-Series Analysis to Assess Mid- and Long-Term Recharge Model Changes Due to Multiple Strong Seismic Events in Carbonate Aquifers. Water 2020, 12, 3073.

Fronzi, D.; Gaiolini, M.; Mammoliti, E.; Colombani, N.; Palpacelli, S.; Marcellini, M.; Tazioli, A. Groundwater-Surface Water Interaction Revealed by Meteorological Trends and Groundwater Fluctuations on Stream Water Level. Acque Sotter. Ital. J. Groundw. 2022, 11, 19–28.

Fronzi, D.; Mirabella, F.; Cardellini, C.; Caliro, S.; Palpacelli, S.; Cambi, C.; Valigi, D.; Tazioli, A. The Role of Faults in Groundwater Circulation before and after Seismic Events: Insights from Tracers, Water Isotopes and Geochemistry. Water 2021, 13, 1499.

Fruzzetti, V.M.E.; Segato, D.; Ruggeri, P.; Vita, A.; Sakellariadi, E.; Scarpelli, G. Fenomeni di Instabilità Della Falesia del Monte Conero: Ruolo Dell'assetto Strutturale. In Proceedings of the Incontro Annuale dei Ricercatori di Geotecnica 2011—IARG 2011, Torino, Italy, 4–6 July 2011; pp. 1–6.

Gigli, G.; Casagli, N. Semi-Automatic Extraction of Rock Mass Structural Data from High Resolution LIDAR Point Clouds. Int. J. Rock Mech. Min. Sci. 2011, 48, 187–198.

Gigli, G.; Frodella, W.; Garfagnoli, F.; Morelli, S.; Mugnai, F.; Menna, F.; Casagli, N. 3-D Geomechanical Rock Mass Characterization for the Evaluation of Rockslide Susceptibility Scenarios. Landslides 2014, 11, 131–140.

Gigli, G.; Morelli, S.; Fornera, S.; Casagli, N. Terrestrial Laser Scanner and Geomechanical Surveys for the Rapid Evaluation of Rock Fall Susceptibility Scenarios. Landslides 2014, 11, 1–14.

Giuffrida, A.; Agosta, F.; Rustichelli, A.; Panza, E.; La Bruna, V.; Eriksson, M.; Torrieri, S.; Giorgioni, M. Fracture Stratigraphy and DFN Modelling of Tight Carbonates, the Case Study of the Lower Cretaceous Carbonates Exposed at the Monte Alpi (Basilicata, Italy). Mar. Pet. Geol. 2020, 112, 104045.

Giuffrida, A.; La Bruna, V.; Castelluccio, P.; Panza, E.; Rustichelli, A.; Tondi, E.; Giorgioni, M.; Agosta, F. Fracture Simulation Parameters of Fractured Reservoirs: Analogy with Outcropping Carbonates of the Inner Apulian Platform, Southern Italy. J. Struct. Geol. 2019, 123, 18–41.

Hamm, S.-Y.; Kim, M.; Cheong, J.-Y.; Kim, J.-Y.; Son, M.; Kim, T.-W. Relationship between Hydraulic Conductivity and Fracture Properties Estimated from Packer Tests and Borehole Data in a Fractured Granite. Eng. Geol. 2007, 92, 73–87.

He, L.; Coggan, J.; Francioni, M.; Eyre, M. Maximizing Impacts of Remote Sensing Surveys in Slope Stability. A Novel Method to Incorporate Discontinuities into Machine Learning Landslide Prediction. ISPRS Int. J. GeoInf. 2021, 10, 232.

Iadanza, C.; Trigila, A.; Vittori, E.; Serva, L. Landslides in Coastal Areas of Italy. Geol. Soc. Lond. Spec. Publ. 2009, 322, 121–141.

International Society for Rock Mechanics Commission on Standardization of Laboratory and Field Tests. Suggested Methods for the Quantitative Description of Discontinuities in Rock Masses. Int. J. Rock Mech. Min. Sci. Geomech. Abstr. 1978, 15, 319–368.

Jablonska, D.; Pitts, A.; Di Celma, C.; Volatili, T.; Alsop, G.I.; Tondi, E. 3D Outcrop Modelling of Large Discordant Breccia Bodies in Basinal Carbonates of the Apulian Margin, Italy. Mar. Pet. Geol. 2021, 123, 104732.

James, M.R.; Chandler, J.H.; Eltner, A.; Fraser, C.; Miller, P.E.; Mills, J.P.; Noble, T.; Robson, S.; Lane, S.N. Guidelines on the Use of Structure-from-motion Photogrammetry in Geomorphic Research. Earth Surf. Process. Landf. 2019, 44, 2081–2084.

Jia, L.; Cai, J.; Wu, L.; Qin, T.; Song, K. Influence of Fracture Geometric Characteristics on Fractured Rock Slope Stability. Appl. Sci. 2023, 13, 236.

Karra, S.; O'Malley, D.; Hyman, J.D.; Viswanathan, H.S.; Srinivasan, G. Modeling Flow and Transport in Fracture Networks Using Graphs. Phys. Rev. E 2018, 97, 033304.

Karatalov, N., Stefaniak, A., & Vaughan, L. (2017). DFN Modeling Aided Reservoir Characterization. Abu Dhabi International Petroleum Exhibition & Conference.

Kemeny, J.; Post, R. Estimating Three-Dimensional Rock Discontinuity Orientation from Digital Images of Fracture Traces. Comput. Geosci. 2003, 29, 65–77.

Korneva, I., Cilona, A., Tondi, E., Agosta, F., & Giorgioni, M. (2015). Characterisation of the permeability anisotropy of Cretaceous platform carbonates by using 3D fracture modelling: The case study of Agri Valley fault zones (southern Italy).

Krzeminska, D.M.; Bogaard, T.A.; Malet, J.-P.; Van Beek, L.P.H. A Model of Hydrological and Mechanical Feedbacks of Preferential Fissure Flow in a Slow-Moving Landslide. Hydrol. Earth Syst. Sci. 2013, 17, 947–959.

Krzeminska, D.M.; Bogaard, T.A.; Van Asch, T.W.; Van Beek, L.P.H. A Conceptual Model of the Hydrological Influence of Fissures on Landslide Activity. Hydrol. Earth Syst. Sci. 2012, 16, 1561–1576.

Lato, M.; Diederichs, M.S.; Hutchinson, D.J.; Harrap, R. Optimization of LiDAR Scanning and Processing for Automated Structural Evaluation of Discontinuities in Rockmasses. Int. J. Rock Mech. Min. Sci. 2009, 46, 194–199.

Laux, D.; Henk, A. Terrestrial Laser Scanning and Fracture Network Characterisation–Perspectives for a (Semi-) Automatic Analysis of Point Cloud Data from Outcrops. Z. Dtsch. Ges. Für Geowiss. 2015, 166, 99–118.

Lei, Q.; Latham, J.-P.; Tsang, C.-F. The Use of Discrete Fracture Networks for Modelling Coupled Geomechanical and Hydrological Behaviour of Fractured Rocks. Comput. Geotech. 2017, 85, 151–176.

Leucci, G.; Persico, R.; De Giorgi, L.; Lazzari, M.; Colica, E.; Martino, S.; Iannucci, R.; Galone, L.; D'Amico, S. Stability Assessment and Geomorphological Evolution of Sea Natural Arches by Geophysical Measurement: The Case Study of Wied Il-Mielah Window (Gozo, Malta). Sustainability 2021, 13, 12538.

Li, X.; Liu, J.; Gong, W.; Xu, Y.; Bowa, V.M. A Discrete Fracture Network Based Modeling Scheme for Analysing the Stability of Highly Fractured Rock Slope. Comput. Geotech. 2022, 141, 104558.

Loiotine, L.; Liso, I.S.; Parise, M.; Andriani, G.F. Optimization of Geostructural Surveys in Rock Mass Stability Analyses Using Remote Sensing Techniques. Ital. J. Eng. Geol. Environ. 2019, 73–78.

Makedonska, N.; Jafarov, E.; Doe, T.; Schwering, P.; Neupane, G. EGS Collab Team Simulation of Injected Flow Pathways in Geothermal Fractured Reservoir Using Discrete Fracture Network Model. In Proceedings of the 45th Workshop on Geothermal Reservoir Engineering, Stanford, CA, USA, 10–12 February 2020; pp. 10–12.

Maffucci, R., Bigi, S., Corrado, S., Chiodi, A., Di Paolo, L., Giordano, G., & Invernizzi, C. (2015). Quality assessment of reservoirs by means of outcrop data and "discrete fracture network" models: The case history of Rosario de La Frontera (NW Argentina) geothermal system. Tectonophysics, 647–648, 112–131.

Mammoliti, E.; Fronzi, D.; Cambi, C.; Mirabella, F.; Cardellini, C.; Patacchiola, E.; Tazioli, A.; Caliro, S.; Valigi, D. A Holistic Approach to Study Groundwater-Surface Water Modifications Induced by Strong Earthquakes: The Case of Campiano Catchment (Central Italy). Hydrology 2022, 9, 97.

Mammoliti, E.; Stefano, F.D.; Fronzi, D.; Mancini, A.; Malinverni, E.S.; Tazioli, A. A Machine Learning Approach to Extract Rock Mass Discontinuity Orientation and Spacing, from Laser Scanner Point Clouds. Remote Sens. 2022, 14, 2365.

Massaro, L.; Corradetti, A.; Vinci, F.; Tavani, S.; Iannace, A.; Parente, M.; Mazzoli, S. Multiscale Fracture Analysis in a ReservoirScale Carbonate Platform Exposure (Sorrento Peninsula, Italy): Implications for Fluid Flow. Geofluids 2018, 2018, 7526425.

Massaro, L., Corradetti, A., Tramparulo, F. d'Assisi, Vitale, S., Prinzi, E. P., Iannace, A., Parente, M., Invernizzi, C., Morsalnejad, D., & Mazzoli, S. (2019). Discrete Fracture Network Modelling in Triassic–Jurassic Carbonates of NW Lurestan, Zagros Fold-and-Thrust Belt, Iran.

Mayolle, S.; Soliva, R.; Dominguez, S.; Wibberley, C.; Caniven, Y. Nonlinear Fault Damage Zone Scaling Revealed through Analog Modeling. Geology 2021, 49, 968–972.

Montanari A.; Mainiero M.; Coccioni R.; Pignocchi G. Catastrophic landslide of medieval Portonovo (Ancona, Italy). 2016.

Neuman, S.P. Trends, Prospects and Challenges in Quantifying Flow and Transport through Fractured Rocks. Hydrogeol. J. 2005, 13, 124–147.

Nyberg, B.; Nixon, C.W.; Sanderson, D.J. NetworkGT: A GIS Tool for Geometric and Topological Analysis of Two-Dimensional Fracture Networks. Geosphere 2018, 14, 1618–1634.

Ortega, O.J.; Marrett, R.A.; Laubach, S.E. A Scale-Independent Approach to Fracture Intensity and Average Spacing Measurement. AAPG Bull. 2006, 90, 193–208.

Pan, Y.; Wu, G.; Zhao, Z.; He, L. Analysis of Rock Slope Stability under Rainfall Conditions Considering the Water-Induced Weakening of Rock. Comput. Geotech. 2020, 128, 103806.

Panza, E.; Sessa, E.; Agosta, F.; Giorgioni, M. Discrete Fracture Network Modelling of a Hydrocarbon-Bearing, Oblique-Slip Fault Zone: Inferences on Fault-Controlled Fluid Storage and Migration Properties of Carbonate Fault Damage Zones. Mar. Pet. Geol. 2018, 89, 263–279.

Pepi, A. The role of fracturing in defining the kinematics of rock slope failure and water circulation on the coastal cliff of Ancona. 2021.

Petroleum Experts. Move. 2019. Available online: https://www.petex.com/ (accessed on 2 August 2022).

Pierantoni, P.; Deiana, G.; Galdenzi, S. Stratigraphic and Structural Features of the Sibillini Mountains (Umbria-Marche Apennines, Italy). Ital. J. Geosci. 2013, 132, 497–520.

Pitts, A.D.; Casciano, C.I.; Patacci, M.; Longhitano, S.G.; Di Celma, C.; McCaffrey, W.D. Integrating Traditional Field Methods with Emerging Digital Techniques for Enhanced Outcrop Analysis of Deep-Water Channel-Fill Deposits. Mar. Pet. Geol. 2017, 87, 2–13.

Price, J. Implications of Groundwater Behaviour on the Geomechanics of Rock Slope Stability. In Proceedings of the APSSIM 2016: Proceedings of the First Asia Pacific Slope Stability in Mining Conference, Brisbane, WLS, Australia, 4–6 September 2016; pp. 25–48.

Pringle, J.K.; Westerman, R.; Gardiner, A.R. Virtual Geological Outcrops-Fieldwork and Analysis Made Less Exhaustive? Geol. Today 2004, 20, 64–69.

Riquelme, A.J.; Abellán, A.; Tomás, R. Discontinuity Spacing Analysis in Rock Masses Using 3D Point Clouds. Eng. Geol. 2015, 195, 185–195.

Rocscience. DIPS. 2018. Available online: http://www.rocscience.com (accessed on 11 May 2018).

Romano, V.; Bigi, S.; Carnevale, F.; Hyman, J.D.; Karra, S.; Valocchi, A.J.; Tartarello, M.C.; Battaglia, M. Hydraulic Characterization of a Fault Zone from Fracture Distribution. J. Struct. Geol. 2020, 135, 104036.

Sanderson, D.J.; Nixon, C.W. Topology, Connectivity and Percolation in Fracture Networks. J. Struct. Geol. 2018, 115, 167–177.

Schilirò, L.; Robiati, C.; Smeraglia, L.; Vinci, F.; Iannace, A.; Parente, M.; Tavani, S. An Integrated Approach for the Reconstruction of Rockfall Scenarios from UAV and Satellite-Based Data in the Sorrento Peninsula (Southern Italy). Eng. Geol. 2022, 308, 106795.

Seers, T.D.; Sheharyar, A.; Tavani, S.; Corradetti, A. Virtual Outcrop Geology Comes of Age: The Application of Consumer-Grade Virtual Reality Hardware and Software to Digital Outcrop Data Analysis. Comput. Geosci. 2022, 159, 105006.

Smeraglia, L.; Mercuri, M.; Tavani, S.; Pignalosa, A.; Kettermann, M.; Billi, A.; Carminati, E. 3D Discrete Fracture Network (DFN) Models of Damage Zone Fluid Corridors within a Reservoir-Scale Normal Fault in Carbonates: Multiscale Approach Using Field Data and UAV Imagery. Mar. Pet. Geol. 2021, 126, 104902.

Studi Geologici Camerti. Dipartimento di Scienze della Terra. Università degli Studi di Camerino. Volume Speciale “La geologia delle Marche”, 1986, 9-27, 35-55, 61-81, 89-90, 91-98, 99-103, 135-145.

Sturzenegger, M.; Stead, D. Close-Range Terrestrial Digital Photogrammetry and Terrestrial Laser Scanning for Discontinuity Characterization on Rock Cuts. Eng. Geol. 2009, 106, 163–182.

Terzaghi, R.D. Sources of Error in Joint Surveys. Geotechnique 1965, 15, 287–304.

Tuckey, Z. An Integrated UAV Photogrammetry-Discrete Element Investigation of Jointed Triassic Sandstone near Sydney, Australia. Eng. Geol. 2022, 297, 106517.

Vasarhelyi, B.; Ván, P.J.E.G. Influence of water content on the strength of rock. Eng. Geol. 2006, 84, 70–74.

Volatili, T.; Agosta, F.; Cardozo, N.; Zambrano, M.; Lecomte, I.; Tondi, E. Outcrop-Scale Fracture Analysis and Seismic Modelling of a Basin-Bounding Normal Fault in Platform Carbonates, Central Italy. J. Struct. Geol. 2022, 155, 104515.

Volatili, T.; Zambrano, M.; Cilona, A.; Huisman, B.A.H.; Rustichelli, A.; Giorgioni, M.; Vittori, S.; Tondi, E. From Fracture Analysis to Flow Simulations in Fractured Carbonates: The Case Study of the Roman Valley Quarry (Majella Mountain, Italy). Mar. Pet. Geol. 2019, 100, 95–110.

Walter, C.; Faraj, F.; Fotopoulos, G.; Braun, A. Augmenting Geological Field Mapping with Real-Time, 3-D Digital Outcrop Scanning and Modeling. Geosphere 2022, 18, 762–779.

Wei, M.; Dai, F.; Ji, Y.; Wu, W. Effect of Fluid Pressure Gradient on the Factor of Safety in Rock Stability Analysis. Eng. Geol. 2021, 294, 106346.

Wenli, Y.; Sharifzadeh, M.; Yang, Z.; Xu, G.; Fang, Z. Assessment of Fracture Characteristics Controlling Fluid Flow Performance in Discrete Fracture Networks (DFN). J. Pet. Sci. Eng. 2019, 178, 1104–1111.

Worthington, S.R. Estimating Effective Porosity in Bedrock Aquifers. Groundwater 2022, 60, 169–179.

Zhang, Q.-H.; Yin, J.-M. Solution of Two Key Issues in Arbitrary Three-Dimensional Discrete Fracture Network Flow Models. J. Hydrol. 2014, 514, 281–296.